Optimisation of a flow cytometry antibody panel to detect BCG-induced innate responses in infants.

Author: Temwa – **Dango** Mwambene

Supervisor: Professor Thomas J. Scriba

Co-Supervisor: Dr Anele Gela

MSc (Med) in Clinical Sciences and Immunology

In the Division of Immunology, Department of Pathology

Faculty of Health Sciences

University of Cape Town

Plagiarism declaration

I know that plagiarism is wrong. Plagiarism is to use another's work and pretend that it is one's own.

I have used the American Society for Microbiology Journal citation style for citation and referencing. Each contribution to, and quotation in, this thesis from the work(s) of other people has been attributed and has been cited and referenced.

This thesis is my own work. I have not allowed and will not allow anyone to copy my work with the intention of passing it off as their own work.

I empower the university to reproduce for the purpose of research either the whole or any portion of the contents in any manner whatsoever.

Signed by candidate

Signature: Temwa - Dango Mwambene Date: 2022-02-11

Abstract

The outcome after exposure to *Mycobacterium tuberculosis* is highly variable ranging from clearance, latency to a wide spectrum of subclinical and clinical tuberculosis (TB) disease. The underlying basis of the variable disease outcomes to mycobacterial exposure is largely unknown and is thought to involve a complex interplay between genetic variation in both host and pathogen. This is further convoluted by factors such as age, geography, coinfections including human immunodeficiency virus (HIV) and previous Bacillus Calmette–Guérin (BCG) vaccination. As it stands, other than inborn errors in key mycobacterial susceptibility genes both animal and human studies have not found many genetic polymorphisms that are strongly and reproducibly associated with increased mycobacterial disease susceptibility and/or BCG vaccine efficacy. Given the complexity of the interplay between the variability in disease susceptibility, BCG vaccine efficacy and human exposure to genetically diverse pathogens there is a need to study both host and pathogen genetic factors that contribute to increased TB disease susceptibility. This will facilitate rational design of more broadly efficacious interventions.

This MSc project is nested in a project which aims to uncover the genetic factors that result in variable responses to BCG vaccination and in so doing, expand the basis of learning for novel TB vaccine candidates. The overall aim of this MSc was to optimise a flow cytometry panel to measure the BCG-induced innate immune responses in infants. The innate response to BCG was characterised by whole blood intracellular cytokine staining of banked, previously stimulated immune cells from 25, 10-week-old, HIV-uninfected, infants. The cohort is a subset of participants of a randomised control trial conducted in Worcester, South Africa. A 13-colour flow cytometry antibody panel was successfully optimised for enumerating and measuring cytokine and cell maturation marker expression by neutrophils, monocytes, pDCs, mDCs and T cells in response to BCG stimulation. Expression of cytokines (IFNγ, IL-6, TNF) and maturation markers (CD40, PD-L1) by these cell subsets to BCG stimulation were quantified, allowing identification of single nucleotide polymorphisms that associate with variability in innate responses to BCG.

Results from this MSc thus inform the bigger project which aims to determine genetic determinants of innate responses to BCG and TB disease risk.

Table of Contents

Dedication

I dedicate this thesis to Professor Wendy Burgers. My mentor, friend and real-life Ms Honey. Without her I would not be alive nor well enough to complete this degree – my freedom masters. I am eternally grateful for your kindness, generosity and care.

Acknowledgements

1. Thank you so much to my supervisor Professor Thomas Scriba for believing in me and giving me an opportunity of a lifetime to do my MSc at SATVI. What I learnt at SATVI far extends this thesis. Thank you so much for your academic support, guidance and patience throughout this process. Your commitment to TB immunology is admirable.
2. Thank you so much to my co-supervisor Dr Anele Gela. I am honoured to be the first student you have ever supervised. Thank you for teaching me and walking beside me on every part of this scientific journey.
3. Thank you for everyone at the Cape Town SATVI laboratory. Working with different types of world class scientists and supportive staff has been so formative for me. I will never forget my experience. I cannot think of anyone from the lab who has not helped me along this journey and taught me something. In no particular order thank you so much to Dr Cheleka Mpande, Claire Imbratta, Tessa Lloyd, Cynthia Batyi, Onke Nombida, Dr Nicole Bilek, Yolundi Cloete, Dr Pia Steigler, Lungisa Jaxa, Dr Melissa Murphy, Tim Reid, Mbandi Kimbung, Dr Michelle Fisher, Asma Toefy, Professor Elisa Nemes, Dr Virginie Rozot, Dr Munya Musvosvi, Dr Kate Hadley, Carly Young (my work wife), Mzwandile Erasmus, Miguel Rodo, Rodney Raphela, Simon Mendelsohn, Faheemah Meyer, Ashley Veldsman, Dr Masooda Kaskar, Dr Humphrey Mulenga, Rieyaat Hassiem, Dr Simon Mendelsohn, Dr Agano Kiravu, Professor Mark Hitherill, Constance Schrueder and Alison September.
4. Thank you to Drs Hasse Walum and Desireé De Leon for teaching me how to code in R.
5. Thank you so much to Professors Chris Sassetti and Tom Hawn for my inclusion in this interesting project.
6. Thank you to SATVI and the SAMRC for funding my studies.

7. Thank you so much to my friends for actively cheering me on along this journey: Dr Bakang Taqvi, Pauline Bokea, Sue Nyamnjoh, Kariema Baulackey, Eke Arua.
8. Thank you so much to my thesis writing partner Temhlanga Mndzebele for helping me kickstart my writing.
9. Thank you so much to my sisters, Maka and Mbenecho Mwambene, for inspiring me. Thank you Gogo Hara for scrutinizing my references.
10. Thank you so much to my partner, Dr Mhlengi Mjiyako, for holding my hand to the finish line of this journey.
11. Thank you to every participant and their caregivers for making science like this possible.

List of figures

List of abbreviations

°C - Degree Celsius

% - Percentage

µg - microgram

BCG – Bacillus Calmette–Guérin

BFA – Brefeldin A

BMDM – Bone marrow derived macrophages

CD – Cluster of differentiation

CFU – Colony Forming Units

DCs – Dendritic cells

DMSO – Dimethyl sulfoxide

EDTA – Ethylenediaminetetraacetic acid

FMO – Fluorescence minus one

GWAS – Genetic Wide Association Study

HLA-DR – Human Leukocyte Antigen – DR isotype

ICS – Intracellular cytokine staining

IFNγ/IFNg – Interferon-gamma

IL – Interleukin

IQR – Interquartile range

LPS – Lipopolysaccharide

mDC/mDCs – Myeloid dendritic cell/s

MHC – Major histocompatibility complex

min – Minutes

MFI – Median fluorescence intensity

mL – Millilitres

MSMD – Mendelian Susceptability to Mycobacterial Disease

M. tb – Mycobacterium tuberculosis

NK – Natural killer

pDC/pDCs – Plasmacytoid dendritic cell/s

PBS – Phosphate buffer solution

PD-L1 – Program death ligand-1

RPMI - Roswell Park Memorial Institute Medium

rSD – Robust standard deviation

SATVI – South African TB Vaccine Initiative

SEB – Staphylococcal enterotoxin B

SI – Staining index

SNPs – Single nucleotide polymorphisms

TB – Tuberculosis

Th – T helper

TLR – Toll-like receptor

TNF – Tumor necrosis factor

WHO – World Health Organization

List of tables

Chapter 1: Introduction and literature review

Global epidemiology of Tuberculosis

Tuberculosis (TB) is a communicable disease caused by the bacillus *Mycobacterium tuberculosis* (*M. tb)* which typically affects the respiratory system, but can also affect other systems of the body(1). TB causes an enormous global burden of disease and is, according to the World Health Organisation (WHO), the 13th leading cause of death worldwide in 2019 and the second leading cause of death from a single infectious agent in 2021(1). Of the 1.7 billion people estimated to be latently infected with *M. tb*, only about 5-15% will develop active TB disease with their individual risk increasing considerably with *human immunodeficiency virus* (HIV) co-infection, malnutrition, diabetes, smoking and alcohol consumption(2). Countries with much higher incidence rates of TB are often low- to middle-socioeconomic countries such as South Africa, Kenya and India(1). This is striking as in 2021 the proportion of people with TB and HIV co-infection was highest in the WHO African region.

Much work has been done to study the bacterium and host defences to *M. tb*, to develop and test novel vaccine candidates and to develop new and efficacious therapeutic drugs for treating TB. Despite these efforts, the incidence of new TB cases is not decreasing fast enough to eradicate the epidemic and this is further complicated by the rapidly growing emergence of drug resistant tuberculosis(3). These gains have further been disrupted by the Coronavirus 2019 pandemic(1). Twenty-three percent of the world is estimated to be persistently infected with *M. tb*, although this is based on the prevalence of immunological sensitization and is likely to be an overestimate of the true burden of people with *M. tb* infection(2). *M. tb* is a resilient bacterium and its ability to evade the immune system and establish persistent infection in the human host speaks to the greater than 70 000-year history of co-evolution thought to have existed between the two species(4, 5). Therefore, one of the main immunological challenges in eradicating *M. tb* is due to the bacteria's ability to persist in the host despite strong host immune mechanisms to control and kill the bacteria, posing a challenge to various intervention strategies such as drug treatment programmes, novel vaccine design and TB diagnostics.

Immune response to *M. tb* infection

M. tb is an intracellular pathogen that primarily establishes infections in humans via entry into resident alveolar macrophages in the lung(6).The early, innate immune response to *M. tb* comprises of an aggregation of neutrophils, inflammatory monocytes, alveolar lung macrophages and dendritic cells (DCs) forming immature granulomas and providing a niche for the rapidly expanding bacterial population, particularly in macrophages(7, 8). Macrophages phagocytose *M. tb* and play a vital role in the survival and pathogenesis of *M. tb*, as they are the cellular niche of the bacterium (9). As a result, the immune system focuses most of its effector functions in aiding macrophages to kill the bacterium, particularly T cells, which further activate these macrophages through effector cytokines such as IFNγ and TNF(10). Hence, the innate immune system plays a crucial role in enabling the vital adaptive T cell response to *M. tb*.

Early innate immune responses to *M.tb* begin with primary airway epithelial cells and alveolar macrophages recognizing *M. tb* pathogen-associated molecular patterns via the pattern recognition receptors toll-like receptors (TLR) TLR-2, TLR-4, TLR-6, TLR-9, Retinoic acid-inducible gene-I-like receptors, Nucleotide-binding oligomerization domain-like receptors and C-type lectins(11). This results in the induction of the production of a variety of chemokines and cytokines that mediate the recruitment and activation of other types of immune cells to the lung (11, 12). The epithelial cells have also been found to produce interstitial collagenases, such as the matrix metallopeptidase-1 that drive some of the lung tissue destruction associated with TB disease(11). In *in vivo* and *in vitro* studies airway epithelial cells have been shown to produce nitric oxide and the antimicrobial peptides cathelicidin (LL-37), β-defensin-2, and hepcidin which have all previously been shown to play a crucial role in innate responses against mycobacteria(12). It has also been demonstrated that *M. tb* infected alveolar macrophages change gene expression signatures of bronchial epithelial cells resulting in increased interleukin (IL)-1β expression, further emphasising that epithelial cells are not inert to *M. tb* like previously thought but are part of the dynamic system of cells required to kill mycobacteria(13).

M. tb principally establishes infections in humans via entry into resident alveolar macrophages in the lung (6). Macrophages phagocytose *M. tb* and play a vital role in the survival and pathogenesis of *M. tb* as they are the cellular niche of the bacterium (9). *M. tb* enters macrophages via three types of phagocytosis namely, type I phagocytosis, type II phagocytosis and macropinocytosis; the type utilised is determined by which receptors are activated and affects the survival of the bacterium(14). Once phagocytosed, *M. tb* enters the macrophage in a phagosome which goes through a process of maturation, fusing with acidic lysosomes to form a phagolysosome in which many of the effector killing functions take place, including but not limited to acidic conditions, reactive nitrogen species, reactive oxygen species and exposure to various antimicrobial peptides(15, 16). Macrophages have various mechanisms to limit *M. tb's* access to iron which it needs for survival(17). With the help of CD4+ T cells, macrophages are able to starve *M. tb* by limiting nutrients like tryptophan (18, 19). In lieu of successful intracellular killing of *M. tb* by macrophages, macrophages will either undergo apoptosis or autophagy(20, 21).

Neutrophils, which are defined by the expression of cluster of differentiation (CD)66 or CD16, are an early responder phagocytic killer innate cell and are continually recruited to the site of *M. tb* infection via cytokines and chemokines secreted by regional epithelial cells, alveolar macrophages and other neutrophils who have all been in contact with *M. tb* (12). It has been demonstrated that neutrophils are the most abundant cell type in both sputum and bronchioalveolar lavage samples of active TB patients; these cells also seemed to harbour the highest *M. tb* load(22). The role of neutrophils in clearing an *M. tb* infection is still highly contested in the literature but several interesting phenomena have been noted in conjunction with the classical roles of neutrophils. Neutrophils produce and secrete the antimicrobial enzymes α-defensins, matrix metalloproteases, lactoferrin, and lipocalin to restrict the growth of mycobacteria within macrophages, and promote apoptosis of infected macrophages, thereby limiting *M. tb* survival within the host(12). *M. tb* stimulated neutrophils also secrete chemokines Interferon gamma-induced protein 10, Macrophage Chemoattractant Protein-1, Macrophage Inflammatory Protein-1α/β and pro-inflammatory cytokines tumour necrosis factor (TNF) to recruit and activate other immune cells and enhance macrophage killing(12). Neutrophils work in tandem with macrophages; an example of this is when macrophages phagocytose neutrophils which have undergone apoptosis and utilise their cytotoxic granules - which are colocalised to the phagosome - to thwart the survival of *M. tb* intracellularly(23).

Monocytes are a heterogenous group of innate immune cells that are derived from the bone marrow, circulate in blood and are posited to differentiate in response to infection. Monocytes are defined by relative expressions of CD14 and CD16 expression(24). Using flow cytometry, three phenotypically and functionally monocyte populations have been described, namely classical (CD14++CD16-), intermediate (CD14+CD16+) and non-classical (CD14+CD16++)(24). Classical monocytes make up 80 – 95% of circulating monocytes and are important scavenger cells that are highly phagocytic(24). Intermediate monocytes are 2 – 8% of circulating monocytes and characterised by their production of ROS, their ability to present antigens and participate in the stimulation and proliferation of T cells and other inflammatory responses(24). Non-classical monocytes are 2 -11% of circulating monocytes; they patrol the endothelium for injury and have pro-inflammatory cytokine responses in the context of infection(24). Functional studies have shown that monocytes have two distinct cytokine profiles with a larger population secreting IL-1ß, IL-6, TNF and chemokine ligands 4 whereas, a smaller population secretes granulocyte macrophage-colony stimulating factor, IL-10 and IL-12p40(24).

CD16+ monocytes have been shown to expand in the context of TB infection which resolves with TB treatment suggesting causation by microbial or host components(24). Classical monocytes are thought to be more anti-mycobacterial than non-classical monocytes which have been implicated in promoting bacterial persistence(24). The cytokine profile of monocyte subsets also seems to differ in the context of TB infection. Classical monocytes produce more IL-10 than TNF whereas intermediate and non-classical monocytes produce less IL-10 and more TNF(24). Monocytes may also modulate the immune response by utilising amino acid catabolism; this changes the T cell microenvironment by depleting amino acids and may result in T cell anergy as T cells are sensitive to this(25). Several studies have shown that an increased monocyte to lymphocyte ratio in peripheral blood can be seen as a feature of active TB disease and can predict the risk of active TB disease(24, 25). *M. tb* itself can also affect how monocytes differentiate. Monocytes of active TB patients have been shown to poorly differentiate into DCs affecting antigen presentation(24). *M. tb*, by increasing IL-10 immune regulatory pathways, modulates classical monocytes to differentiate into macrophage phenotypes more permissive for *M. tb* survival(24).

DCs are a diverse population of immune cells that phagocytose pathogens and present their antigens to T cells using major histocompatibility complex (MHC) molecules(26). Dendritic cells are largely classified as myeloid dendritic cells (mDCs) and plasmacytoid dendritic cells (pDCs) which are defined by CD11c and CD123, respectively(27). Different subsets of DCs play varying roles in *M. tb* infection but their individual functions have yet to be well understood. The principal role of DCs during *M. tb* infection is to migrate to draining lymph nodes, present *M. tb* antigens and secrete cytokines in order to activate naïve T cells(26). Thus, DCs play a crucial role in bridging the innate and adaptive immune responses to *M. tb* infection. Migration of DCs to the lymph node is dependent on the upregulation of C-C chemokine receptor type 7 (CCR7) and the secretion of IL-12p40(26, 27). It has been shown that *M. tb* induces the maturation of human DCs and their section of IL-6, IL-12 and TNF(26). Additionally, DCs can also secrete IL-23 and IL-1ß to promote protective T helper (Th) 17 responses against virulent bacterium. There is a paucity on studies investigating the function of pDCs in *M. tb* infection, particularly as they primarily secrete type I interferons(26). pDCs potentially migrate to the site of *M. tb* infection and are thought to work with other DC subsets to influence the T cell response(26, 27).

One of the most important arms of the immune system in eradicating *M. tb* are CD4+ Th1 cells. This is supported by the strong correlation between an increase in TB incidence and HIV co-infection, particularly as the CD4 count of the individual in question diminishes(28). Antigen-specific T helper cells, like other immune cells in the context of *M. tb* infection, primarily function to assist macrophages to become more efficient in killing mycobacteria. *M. tb*-specific T helper cells are primed by dendritic cells that migrate to the draining lymph nodes of the lung(29). The innate response is more immediate whereas the adaptive responses, especially in a host that has not previously been exposed to mycobacteria, requires T cell priming(26). As a result, antigen-specific T cell immunity may require more time to become available at the site of infection(26). Activated CD4+ T cells produce and secrete interferon-gamma (IFNγ) in response to IL-12 signalling from dendritic cells and macrophages(29). IFNγ works in conjunction with TNF, particularly in granulomas, which makes the macrophage environment more hostile for *M. tb* by ensuring the maturation of the phagolysosome endosome, decreasing the pH even further and enhancing the macrophage's ability to produce antimicrobial peptides such as cathelicidin(29, 30).

Other immune cells such as natural killer (NK) cells, mucosal-associated invariant T (MAIT) cells, etc. have also been shown to play a role in the complex immune response to *M. tb* but are not the subject of this Masters in Science (MSc) project(25). Due to the aforementioned lengthy co-evolution between *M. tb* and humans, *M. tb* has the ability to outsmart this complex immune defence strategy(9, 31). Its success as a pathogen can be partially attributed to its ability to survive in alveolar macrophages despite the harsh conditions generated by the collective efforts of various immune cells(16, 31). The pathogen seems to be able to utilise many mechanisms to manipulate various steps of the immune system's attempt to kill it, depending on the context it finds itself in(31).

BCG immunogenicity and efficacy in infants

Bacillus Calmette-Guerin (BCG) is routinely given to infants at birth in most regions of the world(32). It remains the only vaccine licenced to protect against TB. Previous work by our lab, The South African TB Vaccine Initiative (SATVI), in infants has shown that BCG induces polyfunctional CD4+ and CD8+ T cell responses(19,20). Frequencies and functional subsets of this T cell response in blood from BCG-vaccinated infants were not associated with subsequent risk of TB (29, 30). Despite this, it is still necessary to administer BCG to neonates in TB endemic areas as it has been shown to confer reliable protection against childhood forms of severe and/or disseminated TB(32, 33). This protective effect wanes over time resulting in high variability in the efficacy of BCG in protection against pulmonary TB (32, 33). Possible confounders in this variability in efficacy is pre-sensitization with environmental mycobacteria, the administration of genetically different BCG strains, BCG batch differences, route and timing of administration, geography, maternal factors, etc but the evidence for these confounders are not strong(33).

It has been demonstrated that live BCG persists at the site of vaccination for at least 4 weeks(33). The immediate cytokine response to BCG consists of IL-1ß, IL-8, TNF and monocyte chemoattractant protein-1. The cytokine response is biphasic with the initial peak response mediated by local resident cells and a later peak mediated by cells that have migrated to the site(33). The cellular infiltrate consists of monocytes, dendritic cells, lymphocytes and neutrophils(33). Similarly to *M. tb* infection, DCs take up BCG and migrate to lymph nodes and activate T cells(33). BCG induces a Th1 response in adults but either a Th1 or Th2 regulatory response in infants(33). BCG is thought to mediate immunity through the induction of antigen specific memory T cells, but this population of memory cells has yet to be characterised(26, 34). Despite the lack of clarity on the classical memory response to BCG, much more gains have been made to understand the trained innate immunity of BCG. This finding is as a result of observation studies that have shown that infants vaccinated with BCG have a decrease in all-cause mortality risk than those that were unvaccinated(35). Trained innate immunity is the ability of innate immune cells, such as monocytes and NK cells, to respond more rapidly and strongly following immunisation to unrelated antigens to BCG vaccination(35). The main mechanism proposed for this phenomenon is the training of hematopoietic stem cells by BCG(35).

Thus, vaccination with BCG results in activation of dendritic cells and monocytes which secrete cytokines such as IL-12 and IL-18, resulting in the expansion of both classical antigen specific Th1 CD4+ and CD8+ T cells and non-classical cells such as CD1 and HLA-E restricted T cells(36). Although an immune correlate of protection for TB disease is yet to be established, previous work from the genetic host-susceptibility paradigms described above has illuminated that defects in the Th1 pathway, which underlies IL-12-mediated priming of T cells to express IFNγ, other T cell and NK cell defects (GATA2 deficiency) and defects in monocytes and dendritic cells (IRF8 deficiency and CGD), are associated with marked susceptibility to mycobacterial disease(36). Thus, BCG interfaces with most of the known key immune cells and pathways identified in human genetic studies that have been shown to be essential for protection from TB disease.

Genetic susceptibility to Mycobacterial species

The outcome after exposure to *M. tb* is highly variable, ranging from clearance, asymptomatic infection, persistence, to a wide spectrum of subclinical and clinical disease(37). Humans readily encounter various mycobacterial species as they are aerosolised or ingested from the environment: the vast majority of species are free-living saprophytes(38). Exceptions to this is *M. tb* (and *Mycobacterium africanum* and *Mycobacterium bovis* (*M. bovis*), which together form the MTB Complex) which are obligate intracellular pathogens in humans and other mammalian species(38). The high percentage of humans infected with *M. tb* and the greater than 70 000-year history of species co-evolution further suggests that humans are the natural reservoir of this bacterium. In addition, BCG a live-attenuated vaccine from *M. bovis* has a birth coverage rate of ~90% in many countries with high TB disease incidences and an estimated global coverage of 4 billion since its first administration in 1921(32). Thus, humans are exposed variably to mycobacterial species throughout their lifespans and the bacteria cause a wide variety of disease outcomes ranging from ulcers, leprosy to TB (38).

Although the majority of humans will have encountered mycobacterial species, only about 10-15% of individuals will likely end up developing mycobacterial disease, particularly from *M.tb* infection(37, 38). The underlying basis of the variable disease outcomes to *M. tb* exposure is largely unknown and is thought to involve a complex interplay between genetic variation in both host and pathogen and is further convoluted by factors such as age, geography, timing, and co-infections such as HIV and environmental factors(37). Evidence that there is a strong association between genetics and mycobacterial disease outcome comes from studies that have previously shown a higher TB concordance rate in monozygotic versus dizygotic twins and studies of individuals with Mendelian Susceptibility to Mycobacterial Disease (MSMD)(37).

MSMD is a clinical disorder affecting a very rare population of individuals with particular mutations that mediate familial susceptibility to mycobacterial disease(39). Various Mendelian genetic mutations/traits have been elucidated that confer higher susceptibility to mycobacterial disease and infectious diseases in general(38–40). For instance, Casanova et al have described inborn mutations in the Janus Kinases, or Signal Transducer and Activator of Transcription molecules in the IL-12 and IFNγ pathway that are associated with an increased susceptibility to mycobacterial disease(40). Unfortunately, none of this work has yet been able to elucidate more common host genetic factors that are associated with increased mycobacterial disease susceptibility and/or BCG vaccine response efficacy for general populations without MSMD(37–39).

Using a systems genetics approach to TB genomics

As it stands, both the classical inbred murine models and human studies have not enabled identification of many genetic polymorphisms that are strongly and reproducibly associated with increased mycobacterial disease susceptibility and/or BCG vaccine response efficacy for general populations without MSMD(37–39). As Vivek Naranbhai describes it, “limitations in candidate gene studies and early linkage studies made robust identification of specific loci associated with disease challenging, and few loci have been convincingly associated across multiple populations”, but the advent of newer gene expression technologies are providing a way of overcoming these historic challenges (39).

Given the complexity of the interplay between the variability in disease susceptibility, BCG vaccine variable efficacy, the complex immune system and human exposure to genetically diverse pathogens, there is a need to deconvolute these layers of heterogeneity. This can be achieved by investigating both host and pathogen genetic factors that contribute to increased TB disease susceptibility that will facilitate the rational design of more broadly efficacious interventions. This MSc project is a sub-study of such a project, which is a multi-center systems genetics approach to tuberculosis led by Chris Sassetti.

By using combinatorial host and bacterial genetics, the larger project broadly aims to characterise host and pathogen determinants of TB susceptibility and vaccine efficacy in the mouse model and use this as a basis to test hypotheses in human populations. The overall project has a unique approach to murine TB genetic analysis because it incorporates host variation by using a model outbred population consisting of a set of approximately 70, extremely diverse inbred mouse lines termed 'Collaborative Cross' (CC) mice(37). The CC mouse model is a validated inbred mouse model exhibiting a unique and reproducible high genetic diversity and which can be utilised in a myriad of studies(41). This newly generated reference panel captures natural genetic diversity present in outbred populations but allows infinite replication of each genotype. This model is advantageous as it aims to mimic the genetic diversity in human populations.

The human immune genetic work of this project in particular is led by Tom Hawn at the University of Washington in Seattle. The main aim of core is to facilitate the testing of hypotheses that emerge from the mouse genetic data in human cohorts through interactions with several projects. The aim is to find genes and mechanisms in mice and hopefully find SNPs in those genes in humans. In the work that this MSc is part of, the broad objective is to identify genetic determinants of variability in innate responses to BCG. This would be accomplished by using a genome-wide association studies (GWAS) which looks for significant single nucleotide polymorphisms (SNPs) that correlate with variable immune responses. The vaccine response to BCG will be characterized by whole blood intracellular cytokine staining of banked, stimulated immune cells from a previous study of infant BCG vaccination conduced at the South African TB Vaccine Initiative (SATVI), allowing immunological and genetic correlations between human and CC studies to be coordinated.

Current study: Aims and Objectives

Aims of this thesis

The overall aim of this MSc project was to optimise a flow cytometry panel to measure BCG-induced innate immune responses in infants. This panel was developed in order to measure differences in innate immune responses ten weeks after BCG vaccination in infants using flow cytometry and potentially identify SNPs that are associated with innate immune response magnitude or function.

Rationale

Broadly, previous and current work conducted at SATVI focuses on understanding immune responses against *M. tb* during natural *M. tb*-infection or after vaccination. Results from such studies inform the development of new vaccines and innovative assessment of their immunogenicity. To this end, we will contribute to this by potentially uncovering the genetic factors that result in variable infant innate responses to BCG vaccination and in so doing expand the basis of learning for novel TB vaccine candidates.

Objectives of this thesis

I. To develop and optimise a whole blood innate cell intracellular cytokine multi-colour flow cytometry panel to measure innate cell response to BCG.

II. To establish a gating strategy to elucidate consistent T cell, monocyte, myeloid dendritic cell and plasmacytoid dendritic cell and neutrophil responses to BCG vaccination in infants.

III. To measure and define the range in magnitude of pro-inflammatory cytokine and maturation marker responses by innate cells in 25 BCG exposed, ten-week-old infants.

Chapter 2: Optimisation of a thirteen-colour flow cytometric panel to measure BCG-induced cytokine and maturation marker expression on peripheral blood immune cell subsets

Introduction

Our understanding of innate immune cell subtype response to BCG vaccination is not well understood. In order to expand our understanding of the human host immune response to BCG vaccination we need to be able to enumerate the different immune cell subtypes that are responsive to vaccination and characterise the specific functional responses they create. In this project, we are aiming to further understand the innate immune responses in infants to BCG vaccination. Participants were originally recruited into a randomised controlled trial comparing the efficacy of percutaneous and intradermal vaccination with Japanese (Tokyo) 172 BCG in the prevention of TB in infants vaccinated at birth(42).

This is a particular obstacle in our project as the samples we aim to utilise to study these responses are cryopreserved whole blood from an infant cohort. This poses a challenge for three reasons. Firstly, at the time of the original study's recruitment process obtaining large volumes of blood from infants proved to be difficult(43), leaving us with very small volumes of blood to work with. Secondly, the samples were originally stimulated to measure adaptive T cell responses. The longer stimulation duration is not optimal for measuring innate immune responses, which respond more rapidly than T cells. This means that we may potentially miss the peak window in which these innate cells respond to BCG. Thirdly, although these samples were immediately stimulated and fixed at the time of recruitment, they have been cryopreserved in liquid nitrogen for ~20 years, potentially compromising the sample quality.

Despite these challenges, this study aimed to cover a broad range of cell types including T cells, neutrophils, mDCs, pDCs and monocytes. To address this we sought to optimise a multi-colour flow cytometry panel. Flow cytometry is a technology that utilises fluidics to analyse fluorescently-labelled, single-cell suspensions. It leverages different lasers that emit light at distinct wavelengths to excite fluorescent dyes conjugated to monoclonal antibodies specific for cellular proteins, such that high dimensional multiparameter data can be collected in a rapid manner(44). This enables the measurement of phenotypic and functional characteristics of cells at a single-cell level. Flow cytometry assays have been particularly useful in studying the immune system as it has facilitated the study of surface phenotypic markers, maturation/activation markers and cytokine expression patterns of various immune cells with new depth(44–46).

Although flow cytometry is a very powerful tool, the assay requires meticulous optimisation of the various combinations of antibody-fluorochromes. This is because the assay requires the reduction and management of signal to noise ratios between antibody-fluorochromes to increase the precision with which we can ascertain fluorescent signal that correspond to specific cells and/or expression markers(47). The complexity of this optimisation process is even more notable in an antibody panel as large as the one our project aimed to address. In this chapter, we describe the development and optimisation of a 13-colour flow cytometric assay that aimed to measure intracellular expression of key proinflammatory cytokines and maturation markers by T cells, neutrophils, mDCs, pDCs and monocytes in cryopreserved, whole blood infant samples stimulated with BCG or Staphylococcal enterotoxin B (SEB), or left unstimulated.

Rationale for selection of phenotypic and functional markers

The main objective of our project was to measure intracellular expression of key pro-inflammatory cytokines and maturation markers by T cells, neutrophils, mDCs, pDCs and monocytes in a BCG vaccinated infant cohort whose whole blood was drawn at

10 weeks of age and stimulated with BCG or SEB, or left unstimulated. To address this objective we selected the following phenotypic markers: CD3 for defining T cells, CD66 for neutrophils, HLA-DR for the other innate cells of interest, CD33 for myeloid cells, CD11c for mDCs, CD14 for monocytes, CD123 for pDCs, and CD16 to aid in subtyping monocyte populations. We selected TNF, IFNγ and IL-6 as the pro-inflammatory cytokines of relevance and program death ligand-1 (PD-L1) and CD40 as the maturation markers.

Most of these phenotypic and functional markers have already been shown to be effective in elucidating various innate cells in infants for the study of whole blood cytokine responses to mycobacteria in our laboratory(48). CD33 in particular was added due to the phenomenon of CD14 shedding or downregulation on monocytes in response to BCG stimulation(48, 49). By adding CD33, which is a marker for myeloid cells(50), we aimed to circumvent the impact of CD14 reduction on monocytes when defining monocytes, as mature monocytes are defined by CD14.

PD-L1 and CD40 were chosen to measure responses of innate cells to stimulation, a metric that is of particular interest to investigate variability in infant responses to BCG as part of the greater aims of a collaborative project. PD-L1, also called CD274 or B7-H1, is an immunomodulatory marker that interacts with the receptor program death-1 (PD-1)(51). PD-L1 is expressed on a variety of immune cell types and the PD-L1/PD-1 interaction triggers a downstream cascade that upregulates signals that dampens immune effector functioning which enables the chronicity of infections(51). CD40 is an immunomodulatory marker that is a part of the TNF receptor family and is expressed on a variety of immune cell types such as B cells and DCs(52, 53). CD40 and its ligand, CD40-L or gp39, have a very important role in B cells and mediating humoral immunity(52). In the context of monocytes for example, CD40 expression is induced by cytokines such as IFNg and the CD40-CD40L interaction is thought to mediate its cell adhesion to other immune cells to provide co-stimulatory messages that increase their cytokine production(53).

Capacity and configuration of our flow cytometer

We had access to a LSRII flow cytometer (BD Biosciences), a multiparameter instrument configured with red, blue, green and violet lasers. The red laser (633 nm) is configured with three photomultiplier tube detectors, the blue laser (488 nm) with three detectors including side scatter (SSC), the green laser (532 nm) is configured with 5 detectors and the violet laser (405 nm) with 8 detectors. Based on this configuration, the cytometer allows for an 18 colour flow cytometric panel with forward scatter (FSC) and SSC detection. Therefore we can address the aims of our project by utilising a single, large antibody panel.

Rationale for selection of optimal antibody-fluorochrome combinations

The main consideration for the selection of the various antibody-fluorochrome combination in a polychromatic flow cytometric panel relies on leveraging the inherent brightness of a particular fluorochrome and the cell marker density of the marker of interest(45). Typically, the best approach is to utilise an inverse relationship by pairing antibodies specific for markers with the lowest expression levels on the cells of interest, and/or the markers that define the rarer cell subtypes, with the brightest fluorochromes and vice versa(45, 54).

The second most important consideration is the anticipated spectral overlap between the various emission spectra of the potential fluorochromes(45, 47, 54). To this end we utilised ThermoFischer's online flow cytometry panel builder tool, which allowed us to input the parameters of our flow cytometer and the markers we were interested in to gauge what the best theoretical antibody-fluorochrome options would be(55). The final selection relied on this theoretical knowledge, the practical, prior experience of certain markers by members of our laboratory and commercial supplier availability.

Materials and methods

Study participants and blood collection

The study protocol was approved by the Human Research Ethics Committee (HREC) of the University of Cape Town (HREC ref: 571/2021). Healthy adults, between the ages of 18-50 years, were recruited at the SATVI laboratory in Cape Town region of South Africa. Participants provided written informed consent. The exclusion criteria included pregnancy, HIV-1 infection, *M.tb* infection, anaemia and any other acute or chronic infections. Eligible and willing participants were then enrolled and heparinised whole blood samples collected by a trained phlebotomist.

Antigens, whole blood stimulation and cryopreservation

1 mL of adult whole blood was stimulated with either plain media, BCG or lipopolysaccharide (LPS) using the SATVI qualified 12 hour whole blood Intracellular Cytokine Staining (ICS) assay in order to replicate the conditions with which the original samples were processed. This whole blood stimulation assay was specifically developed in our lab to study T cell responses in small volumes of infant blood in rural settings(43).

Plain Roswell Park Memorial Institute (RPMI) 1640 Medium (Lonza Biosciences) served as negative control (Unstim). Bacillus Calmette-Guérin (BCG, Danish 1331) was obtained from Statens Serum Institut, Copenhagen. Each lyophilised vial contained 2-8x10^6 colony forming units (CFUs) of BCG, and was reconstituted with RPMI and used at a final concentration of 1.2x10^6 CFU/mL. Ultrapure LPS, isolated from Salmonella Minnesota, a TLR-4 ligand, was our positive control given our laboratory's previous experience with using it as a control for innate studies as it most accurately accounts for the effect of stimulation on CD14 reduction(48, 49). LPS (Invivogen, lot #LSM-39-02) was used at a final concentration of 100ng/mL. 60 µL of the antigen preparation was prepared in 2 mL polypropylene Sarstedt tubes in order to yield the desired final concentrations once blood was added. Then, 2.5 µg/mL of each costimulatory antibodies, anti-CD28 and anti-CD49d (BD Biosciences, San Jose, CA), was added to all conditions, in order to enhance the specific T cell responses.

Blood was incubated with the respective antigens for 7 hours at 37 ºC. 10 μg/mL Brefeldin-A (BFA) (Sigma Aldrich) was added and the cells were incubated for an additional 5 hours at 37 ºC in a programmed water bath. Cells were then harvested within a 10 hour period. 2 mM Ethylenediaminetetraacetic acid (EDTA) (Sigma Aldrich) was added to each tube to detach adherent cells, vortexed at high speed for 10 seconds, incubated at room temperature for 15 minutes (min) and vortexed again. 1 mL of this blood solution was added to 9 mL of FACS Lysing Solution (BD Biosciences) in a 15 mL Falcon tube and incubated at room temperature for 10 min. This was done in order to lyse red blood cells and fix the leucocytes of interest. The cell solution was centrifugated, the supernatant discarded and the cell pellet was reconstituted in a cryosolution of a 1:1 ratio of 20% dimethyl sulfoxide (DMSO) (Sigma Aldrich) in foetal calf serum (Hyclone) and RPMI. The cells were then directly cryopreserved at 80ºC using a stepwise freezing approach in a 'Mr Frosty' unit (Kimix) containing 250 mL Isopropanol.

Whole blood intracellular cytokine staining (ICS) assay

We used a "one step" staining method, previously optimised in our laboratory, to assess the functional profiles of T cells(43). In this assay, fixed, cryopreserved immune cells from stimulated whole blood samples are thawed, washed in phosphate buffered saline (PBS) (BioWhittaker), permeabilised in Perm/Wash Buffer (BD Biosciences), and stained with combinations of monoclonal antibodies conjugated to fluorophores for 1 hour at 4 °C in 50 µL of brilliant stain (BV) buffer (BD Biosciences). Cells are then washed to get rid of excess, unbound antibody and acquired on the flow cytometer. For quality assurance and to mathematically calculate spillover, compensation was done with positive and negative anti-mouse or anti-rat Ig kappa-beads (BD Biosciences) individually stained with each one of the relevant antibody-fluorophores. Cytometer Setting and Tracking (CST) beads (BD Biosciences) were used for daily voltage settings which are centrally quality assured in the flow cytometry facility of the Institute of Infectious Disease and Molecular Medicine.

Antibody titration

We utilised eight two-fold serial dilutions to determine the optimal antibody titer and stained stimulated, whole blood cells as described above. Our starting titer volume was two times the volume recommended by the manufacturer. The goal was to find the saturating titer with minimal background staining of cells that do not express the marker of interest and minimal spillover to other detector channels. The titration data was analysed using dotplots and histograms to ascertain the frequencies and median-fluorescent intensities (MFIs) of the unstimulated and BCG stimulated samples.

We looked for adequate visual separation between negative and positively stained populations. We used this as a basis to determine the frequency of positive vs negative events, the MFIs of the populations and the robust standard deviation (rSD) of the negative population. We calculated the staining index (SI) by obtaining the difference in MFIs between the positive and negative populations and dividing that by two times the rSD of the negative population. The optimal antibody titer was a combinatorial decision based on the saturating titer that yielded the best visual population separation, the SI, the amount of spread into other channels, how it affected the resolution of other markers and cost.

Fluorescence minus one (FMO) experiment

We conducted a fluorescence minus one (FMO) experiment to identify spectral overlap from a set of fully stained samples minus each individual marker into the various detector channels. This is of extreme importance to ascertain the degree of spillover in a panel, particularly as our panel contains many tandem-dye fluorophores that are subject to dissociation, leading to signal in other channels. This was achieved by staining the entire panel and then running that against FMO controls that have one antibody-fluorochrome omitted from the full panel. The omission of an antibody-fluorochrome from the panel allows us to detect secondary signal from the other channels into the empty, primary antibody channel. Zero signal in the empty channel in an FMO indicates no sources of spectral overlap whilst a positive signal detected in the empty channel in an FMO indicates a source of spectral overlap in that channel.

Data analysis

After acquisition of stained samples on the flow cytometer, data were compensated and analysed using FlowJo software (v10.8.1; Treestar). Flow data were exported to Microsoft Excel and then imported to RStudio (v1.2.5033) for further analysis.

Results

Cell surface expression – CD33 and CD11c

Firstly, in order to determine the optimal antibody concentration for each marker on our panel we utilised the titration process described in 2.6.4. **Figure 1** represents the titration of CD33 BV650, as an example. The titration data were analysed as pseudocolour dot plots (**Fig. 1A**) and histograms (**Fig. 1B**) to determine the frequencies and MFIs of stimulated and unstimulated cells stained under the same conditions. Increasing the titer of CD33-BV650 improved the visual separation between the CD33+ population and the CD33- population (**Fig. 1A**). Initially, at the lower titers, like 0.16µL for example, there was poor separation between the two populations. At the intermediate titers there was optimal resolution and then, at the much higher antibody titers, such as >5µL, the negative population began to shift upwards and the resolution began to lessen again. **Figure 1C** represents the SI and the frequencies of the positive population of BCG-stimulated CD33 cells. The frequencies of the positive population reached saturation at 0.31µL whereas the SI peaked between 1.25 and 2.5µL, and decreased significantly at 5µL and 10µL (**Fig. 1C**). Thus, 1.25µL was chosen as optimal antibody volume as it is a saturating titer that provides good visual separation of the myeloid cells in both the Unstim and BCG stimulated cells.

Considerations of how the chosen antibody titers would affect the other channels were also made. For instance, the saturation titer of CD11c BV421 that visually separated the positive and negative populations best and reached saturation via SI (**Fig. 2**) was 1.25µL. In addition to this, 1.25µL was also the titer that had the least spread into the CD40 BV510 channel (**Fig. 2B**). Thus, concatenated files were created for each titration experiment and each titrated antibody was checked to see what degree of spread would occur to other secondary channels and at which titers. This was a visual determination of how much spread a particular antibody may input to another channel detecting another antibody. In cases where the saturating titer would spread heavily into a secondary channel the lower titer was selected.

Innate maturation marker expression – PD-L1

When we titrated the maturation markers, namely PD-L1 and CD40, on myeloid cells and plasmacytoid dendritic cells, we observed that there were no clear delineations between the negative and positive populations despite an increasing antibody titer. In other words the expression patterns did not follow a bimodal distribution (**Fig. 3B**). Rather, we observed a shift in the entire population for most of the antibody titers (**Fig. 3A and 3B**). Additionally, these shifts would not be able to reliably measure the difference in proportions of cells expressing these markers between the BCG stimulated and unstimulated samples. To this end we overlaid the dotplots and histograms of the Unstim and BCG titrations (**Fig. 3A and 3B**) to determine a titer that would give the greatest shift in MFI between the stimulated and unstimulated population distributions. For the much higher titers of anti-PD-L1 antibody, such as 5 and 10µL, PD-L1 expression could be better ascertained by separation of the distributions of the populations between the stimulations (**Fig. 3A and 3B**). Due to this phenomenon, we decided to utilise MFIs, rather than cell frequencies, for the downstream analysis of the maturation markers on these cell populations of interest.

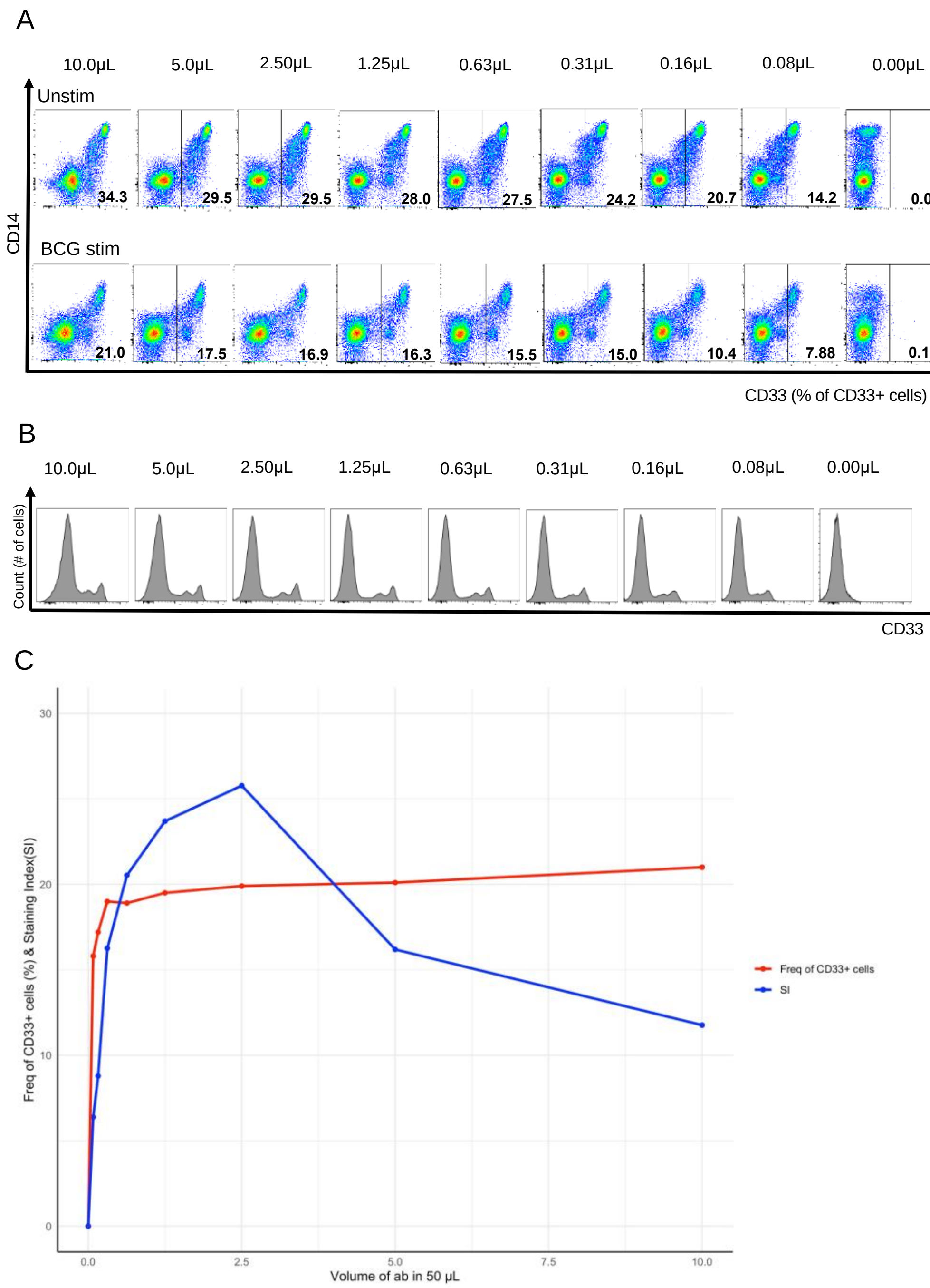

Figure 1. ***Titration of CD33 BV650.*** *Two-fold serial dilutions of CD33 BV650 in adult whole blood stimulated for 12 hours with plain RPMI medium (Unstim) or BCG, displayed as* ***(A)*** *pseudocolor dotplots or* ***(B)*** *histograms (only BCG stimulation represented). The values within each dotplot indicate the percentage of CD33+ cells. The first row of dotplots represent the unstimulated titration and the second the BCG stimulated titration. The values above each dotplot and histogram respectively, indicate the final antibody volume titrated in a 50µL staining reaction.* ***(C)*** *Frequencies of BCG stimulated CD33 positive cells and the staining index (SI) of CD33 BV650 with increasing antibody titer.*

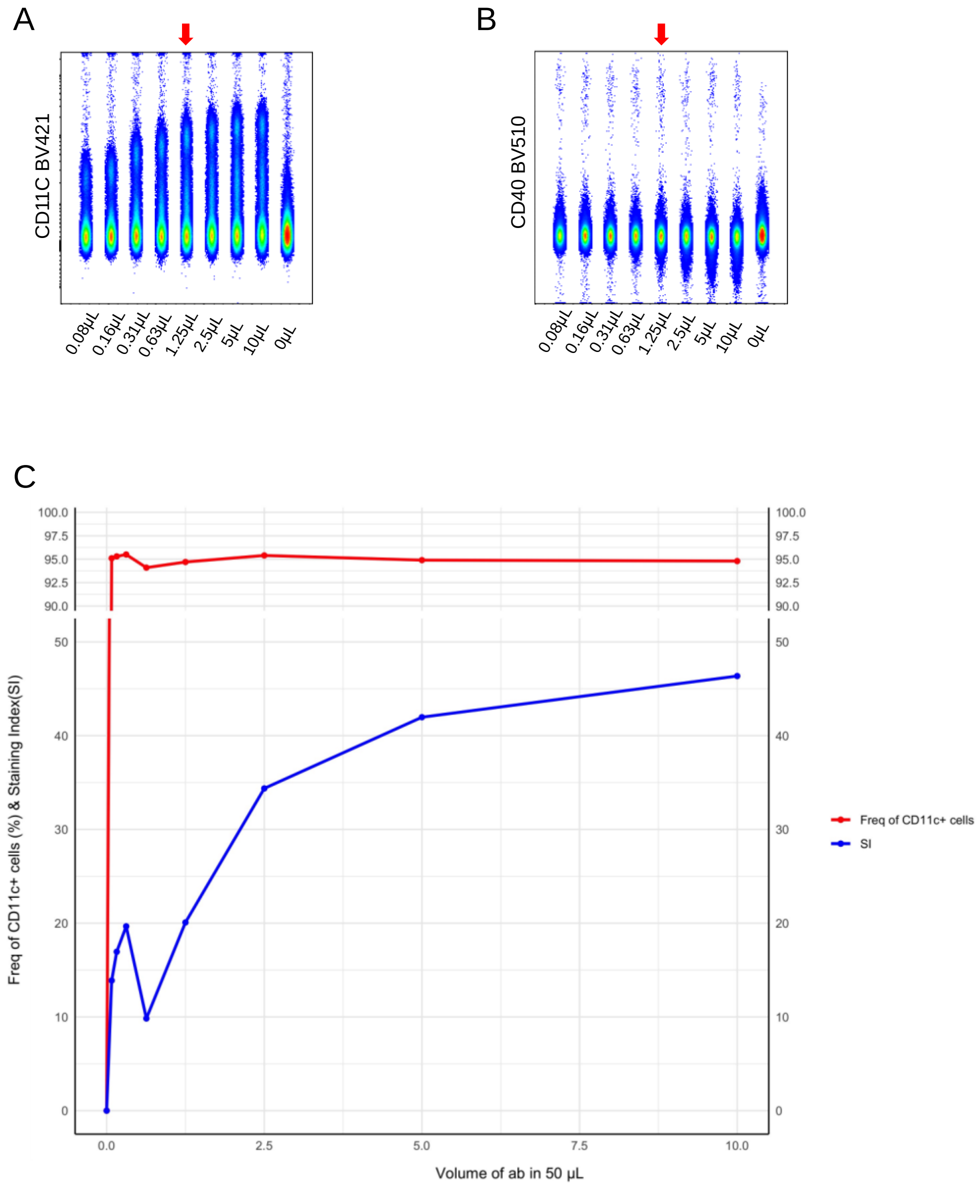

Figure 2. ***Titration of CD11c BV421.*** **(A)** Two-fold serial dilution of CD11c BV421 in adult whole blood stimulated for 12 hours with BCG displayed as concatenated pseudocolor dotplots **(B)** The spread of the various CD11c BV421 titers into the CD40 BV510 secondary channel. The values between the concatenated dotplots indicate the final antibody volume titrated in a 50 µL staining reaction. The red arrow indicates the titer chosen (1.25µL). This is the titration titer that reached antibody saturation with good population separation but has the least amount of negative spread into the CD40 BV510 channel. **(C)** Frequency of CD11c positive cells and the staining index of CD11c BV421 with increasing antibody titer.

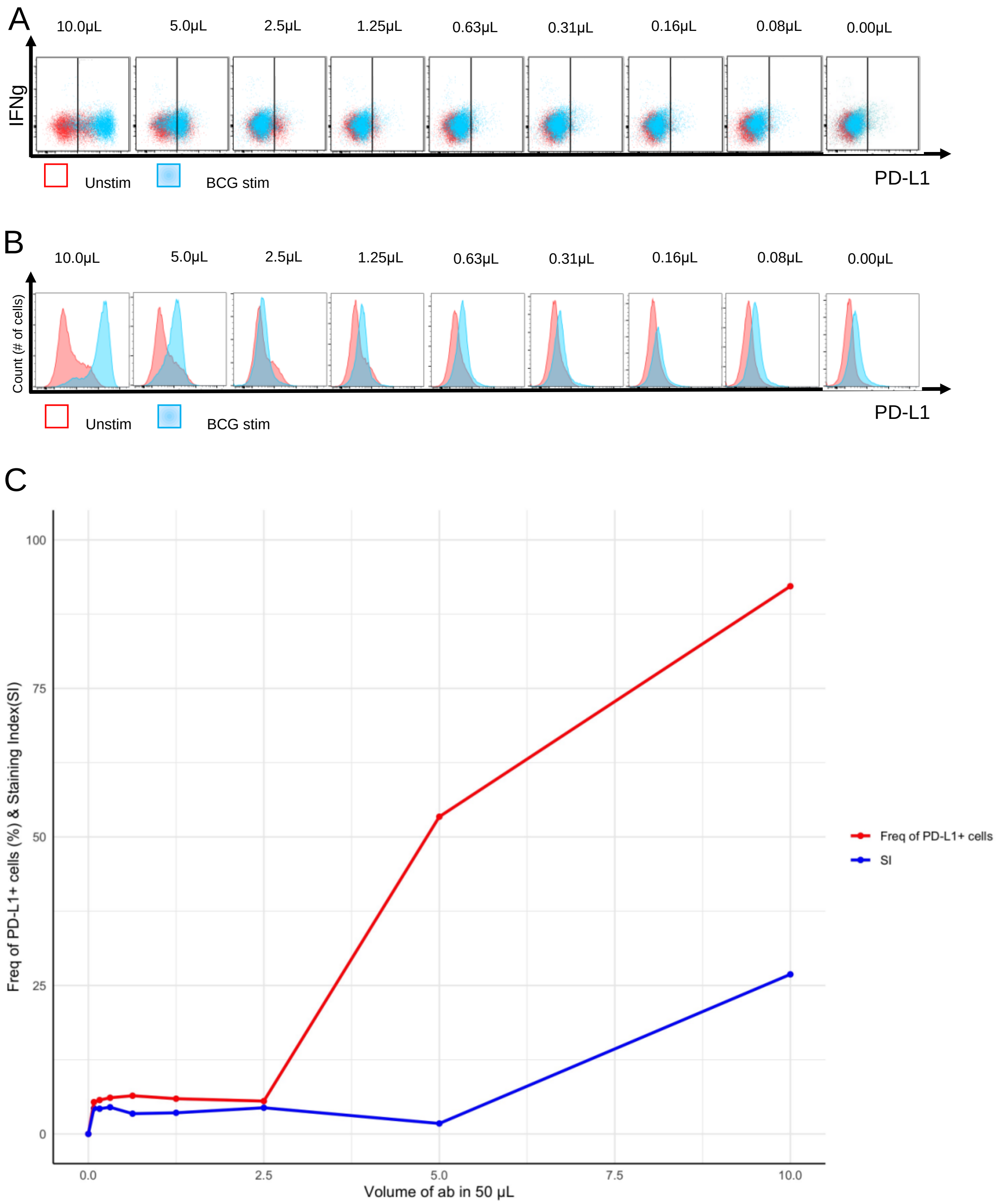

*Figure 3. **Titration of PD-L1 PE.*** Two-fold serial dilution of PD-L1 PE in adult whole blood stimulated for 12 hours with plain RPMI medium (Unstim) or BCG, displayed as **(A)** overlayed pseudocolor dotplots and **(B)** overlayed histograms. The values above each dotplot indicate the final antibody volume titrated in a 50 µL staining reaction. **(C)** Frequency of BCG stimulated PD-L1 positive monocytes and the staining index of PD-L1 PE with increasing antibody titer.

Fluorescence minus one (FMO) analysis

Our FMO analysis was conducted on BCG stimulated cells and the amount of signal for each marker was measured as the frequencies of cells for each relevant population. **Table 1** represents the outcome of this analysis and the values in the shaded boxes represent the percentage of cells that spread into the secondary channels in the FMO control. The range of spread was from 0.00 – 1.14 %. Generally, this showed that the spectral overlap was low but in the case of myeloid cells or assessing their cytokine expression (**Fig. 4B**) or cell maturation marker expression, the overlap was much higher. To this end we were much more cognisant of including non-specific signal when setting gates to define cytokine positive myeloid cells too low. The frequencies of cells detected in each channel were relatively consistent between FMO controls and similar to those stained with the full 13- colour antibody panel (**Table 1**). We concluded that the spectral overlap detected for all 13 channels was acceptable and would not compromise the reliability of the panel to fulfil our objectives.

*Table 1**. Summary of fluorescence minus one (FMO) results.*** Numbers in each cell depict frequencies of cells staining positive for each antibody depicted in rows, when the antibody in each column is omitted. Whole blood from an adult volunteer was stimulated with plain RPMI media or BCG for 12 hours, fixed and harvested. Fixed cells were stained with the optimised 13- colour panel or with FMOs (shaded boxes). The spectral overlap was assessed by investigating the frequencies of cells with or without each single antibody-fluorochrome within the gate. The values in the shaded boxes represent the frequencies of cells in the channel of interest when the antibody is omitted from the full panel which is indicative of the amount of background fluorescence (spectral overlap) in secondary channels.

FM	CD66	CD16	CD14	CD123	CD3	CD33	CD11c	HLA-DR	IFNg	TNF	PD-L1	CD40	IL-6	BCG stim Full panel
CD66	0.05	46.7	46.7	45.8	45.4	45.8	46.3	43.1	45.3	40.7	46.6	42.6	44.9	43.2
CD16	14.8	0.29	9.31	4.74	11.6	7.91	9.27	15.8	8.89	12.9	6.73	8.09	9.95	11.4
CD14	35.6	38.5	1.14	33.6	30.9	14.1	0.52	12.9	36.4	39.5	40.3	32.2	33.9	30.2
CD123	2.33	5.57	4.81	0.03	1.97	5.56	4.58	4.99	5.40	4.59	4.93	3.93	4.77	5.78
CD3	68.5	71.6	71.0	68.7	0.05	70.2	72.7	71.0	74.0	63.0	76.0	70.0	71.4	66.8
CD33	38.5	29.6	27.2	21.8	27.5	0.58	28.8	58.6	29.3	35.5	27.2	21.6	31.6	31.8
CD11c	56.2	51.9	88.4	52.7	58.9	31.2	0.99	45.7	56.2	52.2	50.3	58.8	53.7	63.1
HLA-DR	19.5	35.3	32.0	29.7	10.9	33.0	33.4	0.64	22.0	28.1	37.1	28.6	34.2	29.4
IFNg	0.29	0.49	0.48	0.47	71.4	0.53	0.51	0.43	0.04	0.47	0.51	0.46	0.47	0.50
TNF	0.19	0.12	0.20	0.10	21.4	0.12	0.19	0.07	0.26	0.00	0.21	0.15	0.17	0.06
PD-L1	43.6	45.7	77.3	32.2	38.4	22.2	42.9	37.0	44.1	38.6	0.14	36.0	41.2	28.7
CD40	37.7	35.4	39.2	0.00	34.8	37.7	40.1	0.00	35.3	36.0	36.5	0.23	38.2	32.8
IL-6	47.2	40.2	15.2	39.9	41.6	55.6	25.7	48.1	36.3	39.9	37.8	39.3	0.64	34.9

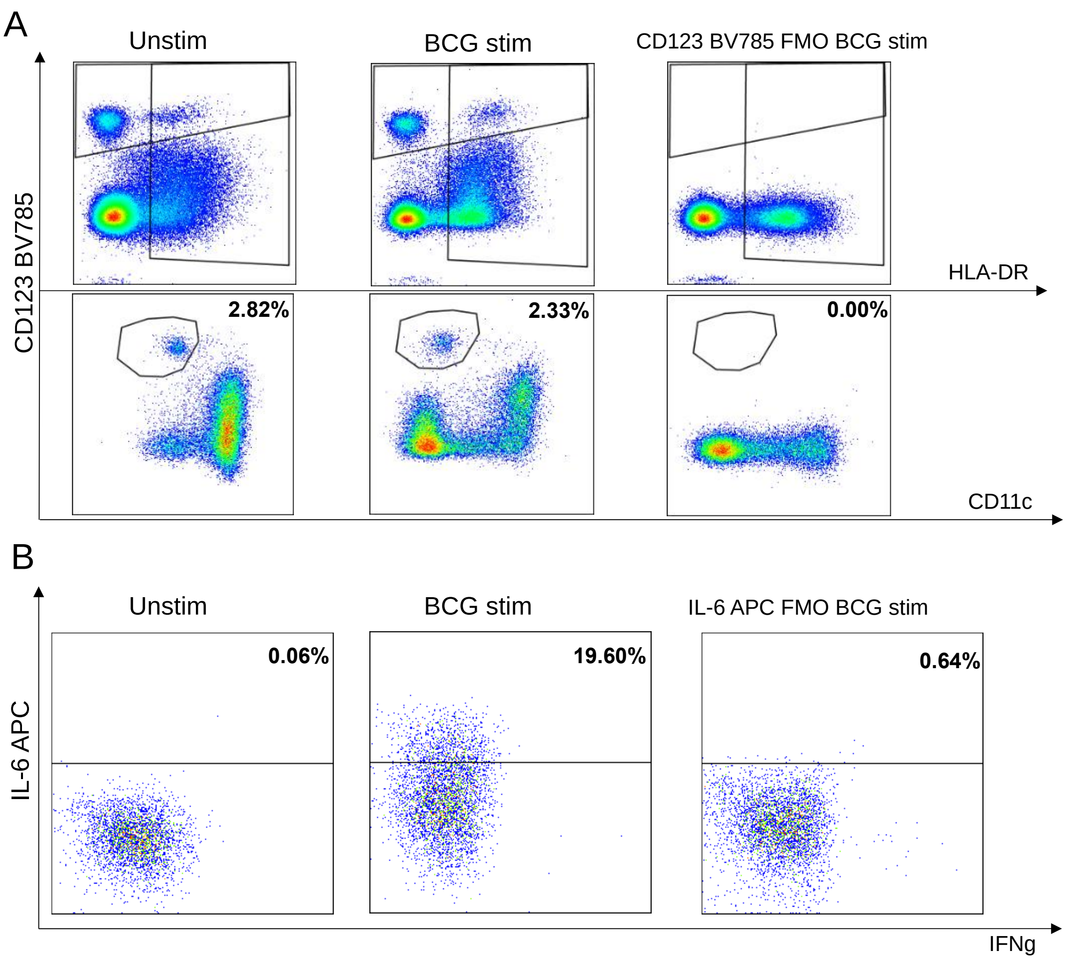

Figure 4. **Fluorescence minus one (FMO) controls. (A)** CD123 BV785 staining for basophils (CD123+HLA-DR-) and plasmacytoid dendritic cells (HLA-DR+CD123+CD11c-). **(B)** IL-6 APC staining for myeloid dendritic cells. There is positive CD123 staining for the unstimulated and BCG stimulated samples stained with the full panel whilst no staining is observed for the FMO control for either CD123+ populations. High background was observed in the IL-6 APC FMO due to the effects of BCG stimulation on myeloid cells; this was accounted for by subsequently shifting the gate higher for the IL-6 positive myeloid cells, so that only true IL-6 expressing cells were included.

Final antibody-fluorochrome panel titers

Table 2 represents the final antibody-fluorochrome titers for the 13-colour panel developed to measure intracellular expression of key pro-inflammatory cytokines and maturation markers by T cells and innate cells. The final titers were selected as a result of the optimisation process described above and combinatorial decision based on the saturating titer that yielded the best visual population separation, the SI, the amount of spread into other channels, how it affected the resolution of other markers and cost. TNF and IFNγ were the only antibodies not titrated as our lab already had historical experience with the identical antibody clone-fluorochrome combinations on the same flow cytometer. These antibody titers were of course included in the FMO experiment to verify their performance in this panel and the full panel was used to stain a test infant sample cohort to ensure that the results were acceptable on cryopreserved infant samples as it did on the adult samples (data not shown).

Table 2. ***Final 13-colour flow cytometric panel with antibody titers.*** Final optimal antibody-fluorochrome titers for a 13-colour innate panel. Information about the clone, supplier and catalog number is also provided.

Marker	Fluorochrome	Clone	Purpose	Titer (uL/50uL)	Supplier (cat #)
CD3	APC H7	SK7	T cells	1.25	BD (560176)
CD66	BV711	B6.2/CD66	Neutrophils	0.40 (1:10)	BD (742687)
CD14	PercP eFlour 710	61D3	Monocytes	0.63	Biolegend (46-0149-41)
CD33	BV650	WM53	Myeloid	1.25	BD (740573)
CD16	AF488	3G8	Monocytes, neutrophils	0.25	Biolegend (302022)
CD123	BV785	6H6	Plasmacytoid DCs	0.65	Biolegend (306031)
CD11c	BV421	3.9	Classical DCs	1.25	Biolegend (301627)
HLA-DR	PE Cy5	L243	DCs, Monocytes	0.20 (1:10)	Biolegend (307607)
TNF	PE Cy7	MAb11	Function	1.20 (1:50)	eBioscience (25-7349-82)
IFNy	AF700	B27	Function	0.63	BD (557995)
IL-6	APC	MQ2-13A5	Function	2.50	BD (561441)
PD-L1/CD274	PE	MIH1	Function	5.00	BD (557924)
CD40	BV510	5C3	Function	2.50	Biolegend (334329)

Gating strategy to identify innate immune cell subsets

Once the panel was optimised, we aimed to address the objective of establishing an optimal gating strategy to elucidate consistent T cell, monocyte, myeloid and plasmacytoid dendritic cell and neutrophil populations and measure their response to BCG stimulation. **Figure 5** shows a representative gating strategy of a BCG stimulated infant sample. We deployed a hierarchical gating strategy that excluded events that are not leukocytes, those with irregular or aberrant staining patterns and populations that are not of primary interest. We therefore only included cell populations of interest as we went down the gating tree. We defined the myeloid cells of interest as HLA-DR+/CD123-/CD33+/CD11c+ cells. It was very challenging to discern between monocytes and mDCs based on their overlapping CD14 (and CD16) expression. (**Fig. 6**). Nevertheless, our panel successfully captured changes in cytokine expression in response to stimulation for our cells of interest (**Fig. 7**).

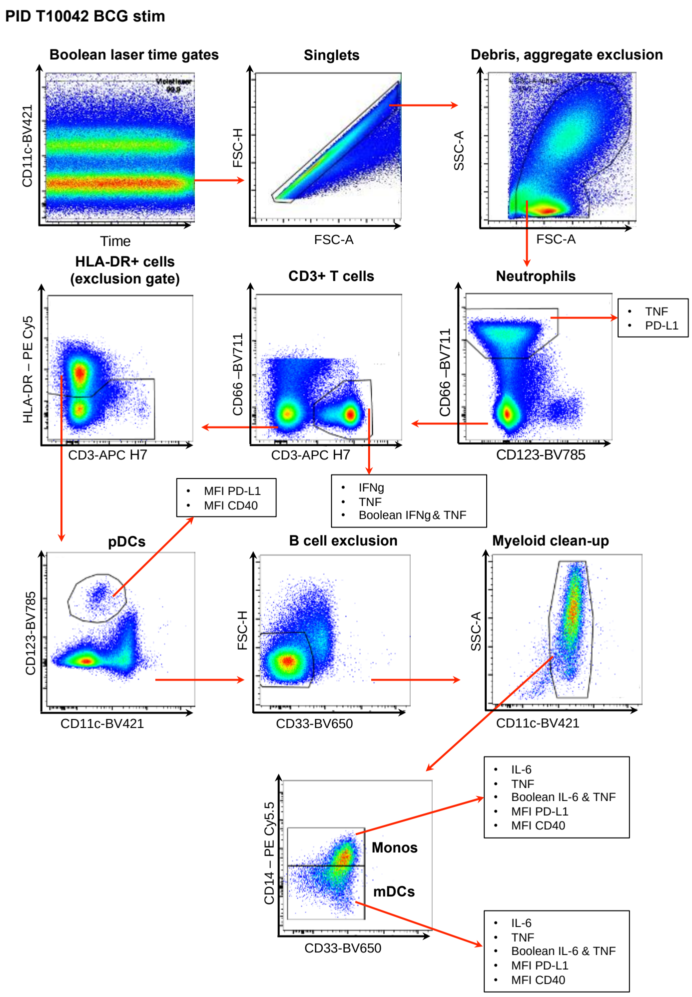

Figure 5. ***Gating strategy for flow cytometry analysis.*** The flow cytometric gating analysis deployed to elucidate consistent T cell, monocyte, myeloid and plasmacytoid dendritic cell and neutrophil populations across samples. This is a representative BCG stimulated sample from an infant (PID T10042). Time gates for each laser were set and Boolean gates used to ensure uniform fluorescence over time during acquisition. Doublets were excluded from the analysis by gating on FSC- height vs FSC-area. Total leucocytes were identified by the SSC-area vs FSC-area gate which excluded additional debris and/or large antibody aggregates. Neutrophils were identified as CD66a/c/e+ cells. The CD66a/c/e- population was used to identify CD3+ T cells. The resultant CD66-CD3- population was used to identify HLA-DR+ cells. pDCs were derived from this compartment and defined as HLA-DR+CD123+CD11c-. B cells were excluded by size and CD33 expression from the other myeloid cells of interest with a FSC-height vs CD33 gate. These myeloid cells were further cleaned up by using a SSC-area vs CD11c gate. Monocytes were separated from mDCs by the use

of CD14. The relevant expression of intracellular cytokines and/or maturation markers was then determined on T cells, neutrophils, monocytes, pDCs and mDCs.

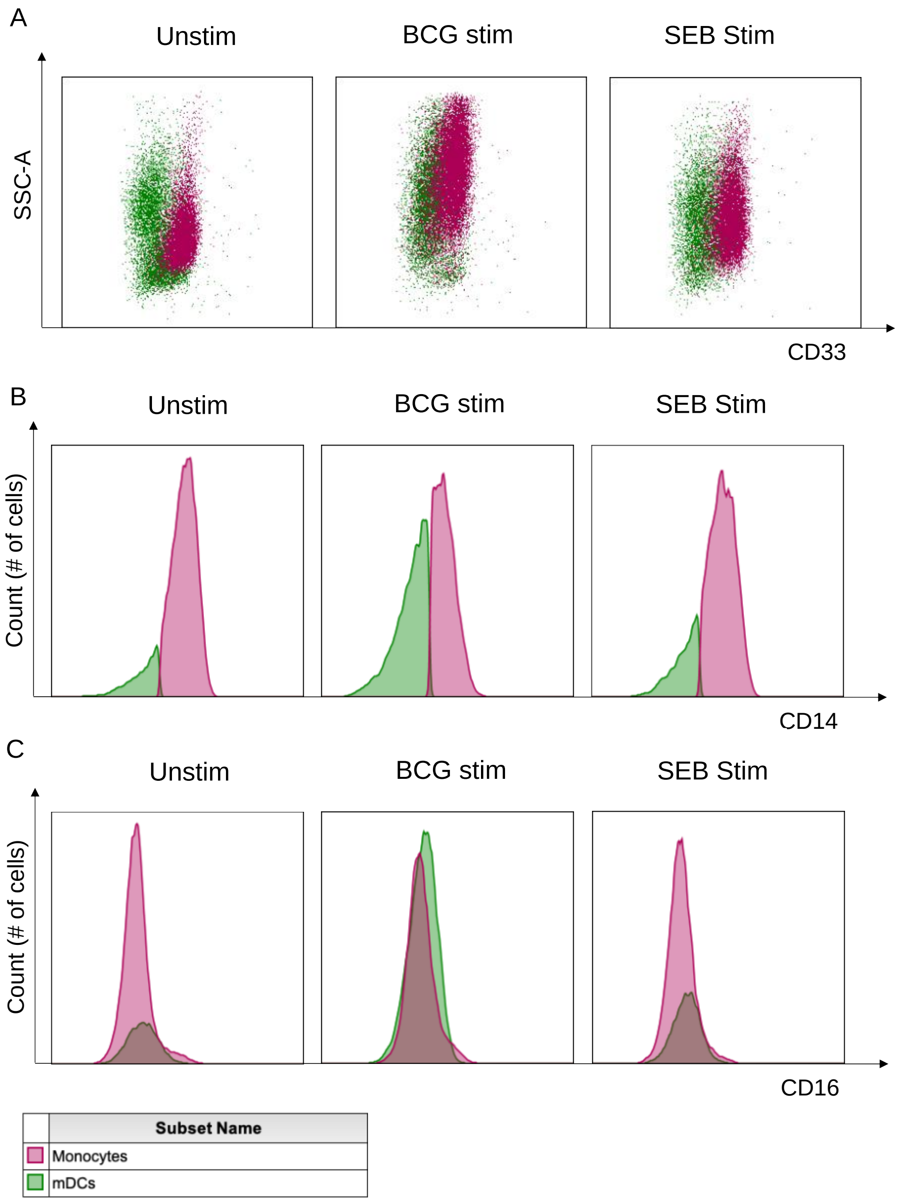

Figure 6. **Challenges in differentiating between monocytes and mDCs.** These myeloid cells were defined as CD33+CD11c+ cells and differentiated by CD14 expression. **(A)** Representative overlaid dotplots of myeloid cells from an infant participant for the three different stimulation conditions is shown. Representative overlaid histogram plots of **(B)** CD14 expression and **(C)** CD16 expression on myeloid cells from an infant participant for the three different stimulation conditions is shown. CD14 expression poorly differentiates between monocytes and mDCs due to the effect of shedding of CD14 on monocytes due to stimulation.

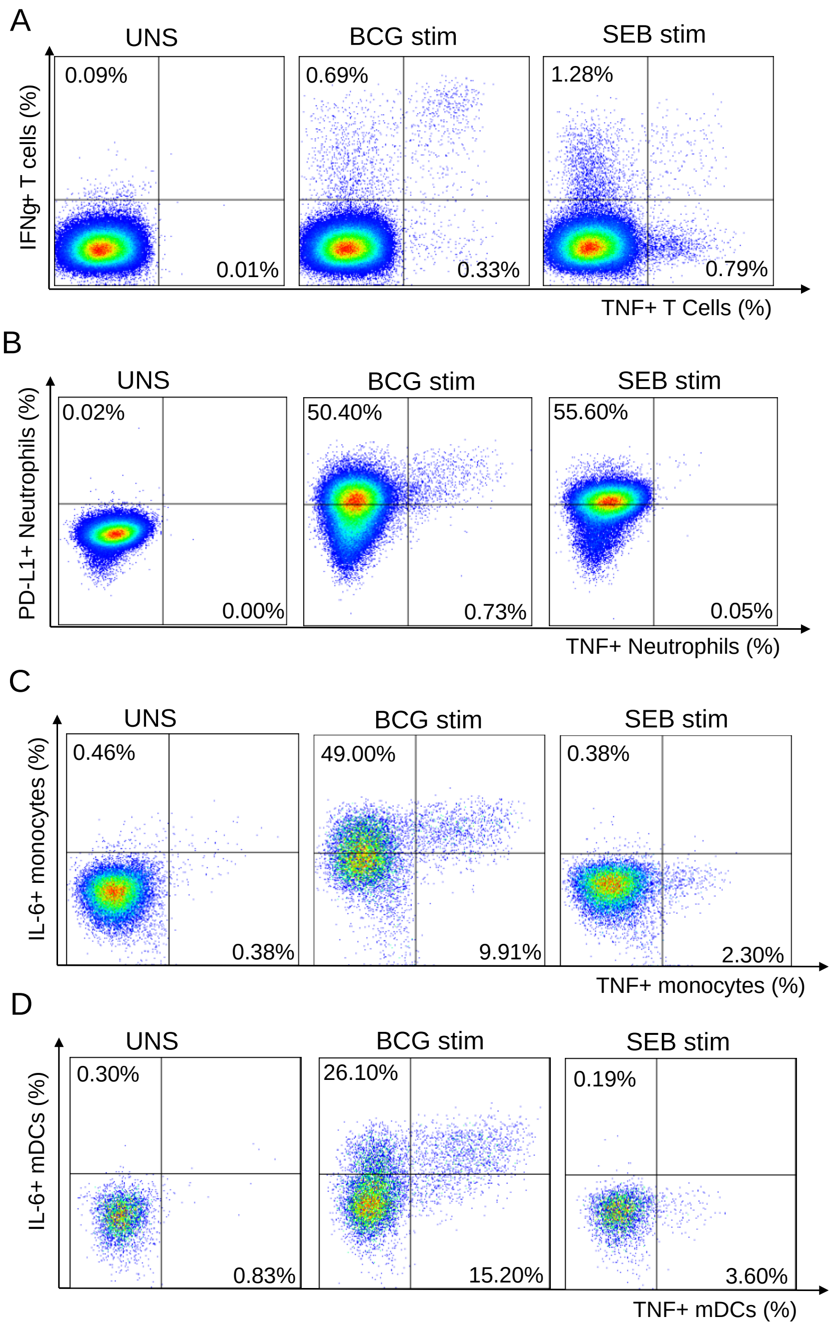

Figure 7. ***Optimised panel successfully captures changes in cytokine expression after BCG or SEB stimulation when compared to Unstim.*** *Whole blood from 22 infant donors was incubated with media (UNS), bacillus Calmette–Guérin (BCG) or Staphylococcal enterotoxin B (SEB) for 12 hours before intracellular cytokine staining and flow cytometric analysis of cell subsets. Cells were then selected and cytokine expression determined based on the gating strategy described in* ***Figure 5****. Representative flow plots of cytokine expression of* ***(A)*** *T cells,* ***(B)*** *Neutrophils,* ***(C)*** *Monocytes,* ***(D)*** *mDCs.*

Discussion

The aim of this chapter was to describe the rationale and report on the necessary experiments that were required to optimise and establish a multiparameter flow cytometric panel that can measure BCG-induced innate immune responses in BCG- or SEB-stimulated infant whole blood samples. This was a particular challenge in our context given that whole blood samples from the cohort of infants we aimed to utilise were already processed and had been stimulated for 12 hours, which is longer than is typically optimal for measuring innate cytokine responses(43, 48). To this end, we described the various meticulous steps undertaken to optimise a 13-colour flow cytometric panel for measuring T cell, monocyte, myeloid and plasmacytoid dendritic cell and neutrophil populations and their response to BCG.

These experiments were undertaken on healthy adult whole blood samples that were stimulated in the exact manner as was done in the original infant. The antibody-fluorochrome combinations selected for our panel were due to the biological characteristics of cells we aimed to study, the laser and detector configuration of the flow cytometer we had access to, practical experience of our laboratory with certain markers and commercial supplier availability. Given that our project is nested in a larger collaborative project our panel needed to lend itself to the needs of the greater project outcomes.

Our laboratory has previously optimised a whole blood intracellular cytokine assay for measuring innate cell responses to live BCG(48). In this assay, the stimulation duration was 6 hours less than what was optimised and stimulated for our cohort of participants(48, 56). Our laboratory has showed that stimulation of whole blood with BCG for a total of 6 hours with the addition of BFA at the three-hour mark was optimal for assessing innate immune outcomes(48). BFA, a fungal metabolite, works by trapping newly synthesised proteins in the endoplasmic reticulum to prevent transport to the Golgi apparatus(57). BFA is primarily used to halt cytokine export out of the cell, allowing newly synthesised proteins to accumulate in the cytoplasm and for these responses to be captured by ICS assays. We were concerned that by having stimulated the cells for a much longer duration and adding BFA at the seven-hour mark, we would have missed the optimal window to capture innate cells cytokine expression, potentially rendering the assay suboptimal for achieving the aims of the project with the pre-stimulated whole blood samples. In addition to this, the dose of BCG inoculum was determined to be an important factor in the response of the innate cells in this study(48). Shey et al showed that the expression of IL-6 was sensitive to BCG inoculum concentration and thus chose 3.6 x 10^5 CFU/mL as the optimal concentration in their study(48). In our study, the samples were optimised for T cell assays and a BCG concentration of 1.2 x 10^6 CFU/mL of lyophilised bacteria was used(43, 56). We were satisfied to see that despite the longer stimulation time and addition of BFA(43), we were still able to successfully capture the responses of these innate cells.

We sequentially titrated each of the commercially obtained antibody-fluorochrome conjugates in order to optimise the reagent panel performance while minimising waste. It is important to titrate antibody-fluorochrome combinations in order to achieve the best signal to noise for each individual flow cytometer since each instrument has different optical, electronic and reagent background noise(45). Too low antibody concentrations result in suboptimal signals and renders the use of the assay to precisely define immune cell populations unreliable. Too high antibody concentrations result in non-specific binding of the antibody and may lead to false positive signals or erroneous results. Typically, the saturating titer corresponded with the titer at which no spread occurred in all the other channels.

When we titrated the PD-L1 and CD40 maturation markers on monocytes, mDCs and pDCs, we observed a continuous expression distribution and a shift in the population between the BCG and SEB stimulated samples relative to the unstimulated samples. To this end we overlaid the dotplots and histograms of the unstimulated and BCG stimulated samples to determine titers that would give us the greatest ability to detect the shift between the stimulated and unstimulated population distributions. Due to this phenomenon, we decided to utilise MFIs, rather than cell frequencies, for the downstream analysis of the maturation markers on these cell populations of interest. Biologically most cell surface markers and cytokines have expression on a continuous spectrum of expression. Although we aim to separate these out into distinct populations using flow cytometry it is not always possible to do this.

We also conducted an FMO experiment in which the full titrated panel is tested in order to identify any background florescence in secondary channels that may result in false positive signals in a particular channel. These may arise due to fluorochrome interactions, excessive spillover or tandem-dye degradation of conjugated fluorochromes that then fluoresce in secondary instead of the primary channel (46). Generally, the spectral overlap was low but in the case of myeloid cells, assessing their cytokine expression and cell maturation marker expression, the signal in secondary channels was much higher. To this end we were much more cognisant of setting gates too low to define cytokine positive myeloid cells when we implemented this gating strategy to measure innate outcomes (Chapter 3).

We faced other challenges, particularly due to marker downregulation by myeloid cells in response to stimulation with BCG. Monocytes, for example, are known to shed CD14, a key lineage marker, from the cell membrane in response to stimulation (49). In our experience this effect was more pronounced with BCG stimulation than LPS or SEB stimulation and makes the identification of monocytes more challenging. We aimed to successfully resolve this with the inclusion of a second myeloid lineage marker, CD33, in our panel. CD33 was less downregulated in response to stimulation and therefore aided in the identification of the myeloid cells of interest. However, it was still challenging to adequately separate the monocyte and mDC populations because of poor resolution of CD14 and other expression markers. Nevertheless, our gating strategy was somewhat able to differentiate between monocytes and mDCs by CD14. Additionally, we found no utilisation for CD16 in the gating strategy in the infant samples despite its utility in defining neutrophils and monocytes subtypes during the panel development and optimisation processes in the adult healthy donor samples.

A major limitation of the flow cytometric assay described here was the absence of a viability marker to exclude dead cells. This would have required an additional staining step with a fixation-resistant viability dye after red cell lysis, but before cell fixation and cryopreservation, to allow exclusion of dead cells(58). Given that this step was omitted in the original sample processing, many years before this project was conceived, we could not make use of a viability dye. The original samples were stimulated on fresh whole blood at that time and a measure of viability of the cells would have been particularly useful to exclude the analysis of dead cells. Nevertheless, very minimal artefactual antibody staining and/or autofluorescence was observed.

In conclusion, our flow cytometry antibody panel is optimised and suitable for enumerating and measuring the cytokine and cell maturation marker expression of neutrophils, monocytes, pDCs, mDCs as well as T cells in response to BCG stimulation.

Chapter 3: Measurement of BCG-induced innate responses in an infant cohort for correlations to genetic analysis

Introduction

This thesis is nested in a larger project aiming to characterise genetic host and pathogen determinants of TB susceptibility and vaccine efficacy, including mechanistic experiments in the novel collaborative cross mouse model, and identification of genetic loci associated with TB disease or BCG vaccination in human populations. The main aim of the project is to facilitate the exploration of the genetic findings in the mouse in human cohorts by pursuing the characterisation of the human BCG response. The vaccine response to BCG will be characterised by whole blood intracellular cytokine staining of banked, stimulated immune cells from a previous SATVI infant cohort, allowing immunological and genetic correlations between human and mouse studies to be identified.

This thesis in particular, will report on the performance of the antibody panel that was optimised in Chapter 2 to measure T cell and innate immune responses in 25 of 200 infants who were given BCG at birth. This cohort of infants has been established to characterise the innate immune response to BCG. We selected a sample size of 25 for the purposes of this MSc project because it is an adequate size to allow an estimation of the magnitude (mean/median) and variability (range) of immune response outcomes to mycobacterial stimulation based on prior studies conducted at our laboratory(43, 48, 58). The aim is to measure the range in variability in the innate immune response of this infant cohort.

Despite the infant samples being originally stimulated for other purposes, we have shown in Chapter 2 that we have optimised a flow cytometry antibody panel suitable for enumerating and measuring the cytokine and cell maturation marker expression of neutrophils, monocytes, pDCs, mDCs as well as T cells in response to BCG stimulation. This enables us to estimate the variability in the innate BCG response. In this chapter, we report on these results for a subset of 25 infants in the cohort.

Genomic deoxyribonucleic acid from peripheral blood mononuclear cells from these same infants have been isolated and sent to Tom Hawn's lab for a GWAS. Ultimately, we intend to correlate the innate immune responses found here to genetic polymorphisms of interest underpinned by the murine work. This will facilitate genetic and mechanistic understandings of BCG vaccine response in a novel paradigm.

This paradigm is best illustrated by motivation for the inclusion of the maturation markers CD40 and PD-L1 in our antibody panel. Using a forward genetic screen our collaborators, in the mouse core of the project, investigated the regulatory pathways in the IFNγ response in a bone marrow derived macrophage (BMDM) line(59). Stimulation of BMDMs with IFNγ upregulated the expression of the co-stimulatory markers MHC II, CD40 and PD-L1(59). Using a CRISPR-Cas9 screen, they were then able to identify the genes that were upregulated in response to expression of these markers and mechanistically implicate complex I of the electron transport chain as a key regulator of IFNγ-gene mediated expression in BMDMs(59). Our hope is that we can investigate correlations between genetic associations like this with BCG vaccination in humans.

Materials and methods

Study participants and blood collection

The study protocol was approved by the human research ethics committee of the university of Cape Town (HREC ref: 571/2021). It is a sub-study of a research project entitled "The role of the innate immune responses, and of genetic determinants of innate immune responses, in BCG-vaccination induced protection against childhood TB" (HREC ref: 332/2005). This MSc thesis describes the data of 25 out of 200 participants. Participants were originally recruited into a randomised controlled trial comparing the efficacy of percutaneous and intradermal vaccination with Japanese

(Tokyo) 172 BCG in the prevention of Tuberculosis in infants vaccinated at birth (HREC ref: 271/2000)(42).

10-week-old infants, who were given BCG at birth, were recruited at the South African Tuberculosis Vaccine Initiative (SATVI) field site in the Worcester region of South Africa. Parents/guardian provided written informed consent. The exclusion criteria included BCG not received at birth within 24 hours, significant perinatal complications, any acute or chronic medical problem, anaemia that was clinically evident, a mother known to be infected with HIV, HIV infection, or any other known form of immune deficiency and intake of systemically immunosuppressive medication, such as oral steroids and a household contact with TB disease, or any person who was coughing. Eligible and consented participants were then enrolled and heparinised whole blood samples collected by a trained phlebotomist.

Antigens, whole blood stimulation and cryopreservation

1 mL of infant whole blood was stimulated and cryopreserved using a qualified 12 hour whole blood ICS assay, as described in Chapter 2. 10 µg/mL SEB (Sigma-Aldrich) was used as a positive stimulation control. Staphylococcal enterotoxin B (SEB) was utilised as a positive control for T cells, as it is a superantigen that is able to activate oligoclonal populations of T cells expressing certain T cell receptor (TCR) β chain variable regions(60). Plain RPMI 1640 medium (Lonza Biosciences) served as negative control (Unstim). Bacillus Calmette-Guérin (BCG, Danish 1331) was obtained from Statens Serum Institut, Copenhagen. Each lyophilised vial contained 2-8 x 10^6 colony forming units (CFUs) of BCG, and was reconstituted with RPMI and used at a final concentration of 1.2 x 10^6 CFU/mL.

Intracellular cytokine staining of banked, stimulated infant whole blood samples

We used a “one step” staining method described in Chapter 2 to enumerate and assess the functional profile of T cells, neutrophils, monocytes, mDCs and pDCs. Samples for all stimulations from each individual infant were stained and acquired in a single batch to reduce variability. The final antibody-fluorochrome titers for the 13-colour panel are listed in **Table 2**.

Data analysis

After acquisition of stained samples on the flow cytometer, data were compensated and analysed using FlowJo software (v10.8.1; Treestar). Flow data were exported to Microsoft Excel and then imported to RStudio (v1.2.5033) for further analysis. The cytokine expression data shown from the stimulated samples was background subtracted using Microsoft Excel; the unstimulated sample was subtracted from the relevant stimulated sample. Negative values were set to zero. Statistical differences of cytokine expression between BCG and SEB stimulated cells were calculated with the Wilcoxon signed rank test. Differences between MFI across the various stimulations were calculated with the Friedman test. Pair-wise comparisons of MFI between stimulation combinations were calculated using the Wilcoxon signed rank test with Holm-Bonferroni correction for multiple comparisons. Correlations were calculated using the Spearman's correlation method. Data were considered statistically significant when $p < 0.05$.

Results

Participants

This thesis describes the variability in BCG-induced responses of 25 infants (among 200 infants for the larger project). A table describing the characteristics of the infant participants is attached in the appendix (**Table A1**). Three of the participants were excluded from the final analysis due to poor sample quality, in accordance with the visual flow cytometric quality control criteria we established. For example, one participant was excluded because there was too much background noise for the unstimulated sample (**Fig. 8**). Thus, this thesis describes data for 22 infant participants. This is the first freeze and thaw cycle for these 20 year old samples. The overall sample exclusion rate of this cycle for the whole cohort is 4% (8/200). This overall exclusion rate is acceptable as it is less than 10%. The higher exclusion rate of 12% reported in the thesis is due to sampling.

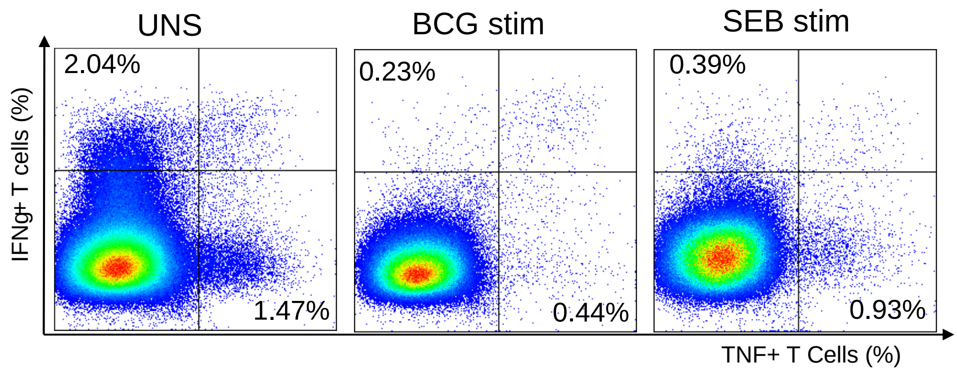

Figure 8. **Representative flow plots of excluded participant.** Representative flow plots of T cell cytokine expression from an infant participant that was excluded from the analysis due to poor sample quality.

Cell counts across cell subsets of interest

Cell counting (or enumeration) is one of the most fundamental measurements and is critical for determining the relative contribution of selected immune cell subsets in a functional assay. Before we could measure the pro-inflammatory response and cell marker maturation expression by innate cells to BCG, we first needed to enumerate our T cell, neutrophil, monocyte, mDC and pDC populations for each infant. It was also important to assess the effect of the BCG or SEB stimulation on the number of cells in order to determine whether stimulation affects our ability to enumerate cells for comparison. For example, Shey et al, showed that BCG stimulation resulted in downregulation or shedding of CD14 making monocyte enumeration challenging and leading to detection of significantly lower frequencies of CD14+ monocytes (48). **Figure 9** illustrates how generally, the range and medians of the number of cells for the various cells of interest, except monocytes, were similar across stimulation conditions. Similarly to Shey et al, we found that monocytes decreased in count in response to stimulation, particularly BCG stimulation(**Fig. 9C**). The median number of unstimulated monocytes was 29700 (Interquartile range (IQR), 18382 – 46523) whereas the BCG stimulated was much lower at a median of 7343 (IQR, 3543 – 12317)(p = 2 x10^4). In our panel, we defined monocytes as CD14+ and thus, a decrease in cell surface expression results in decreased enumeration. Neutrophils also decreased in count in response to simulation but the differences between stimulation conditions were not significant (**Fig. 9B**).

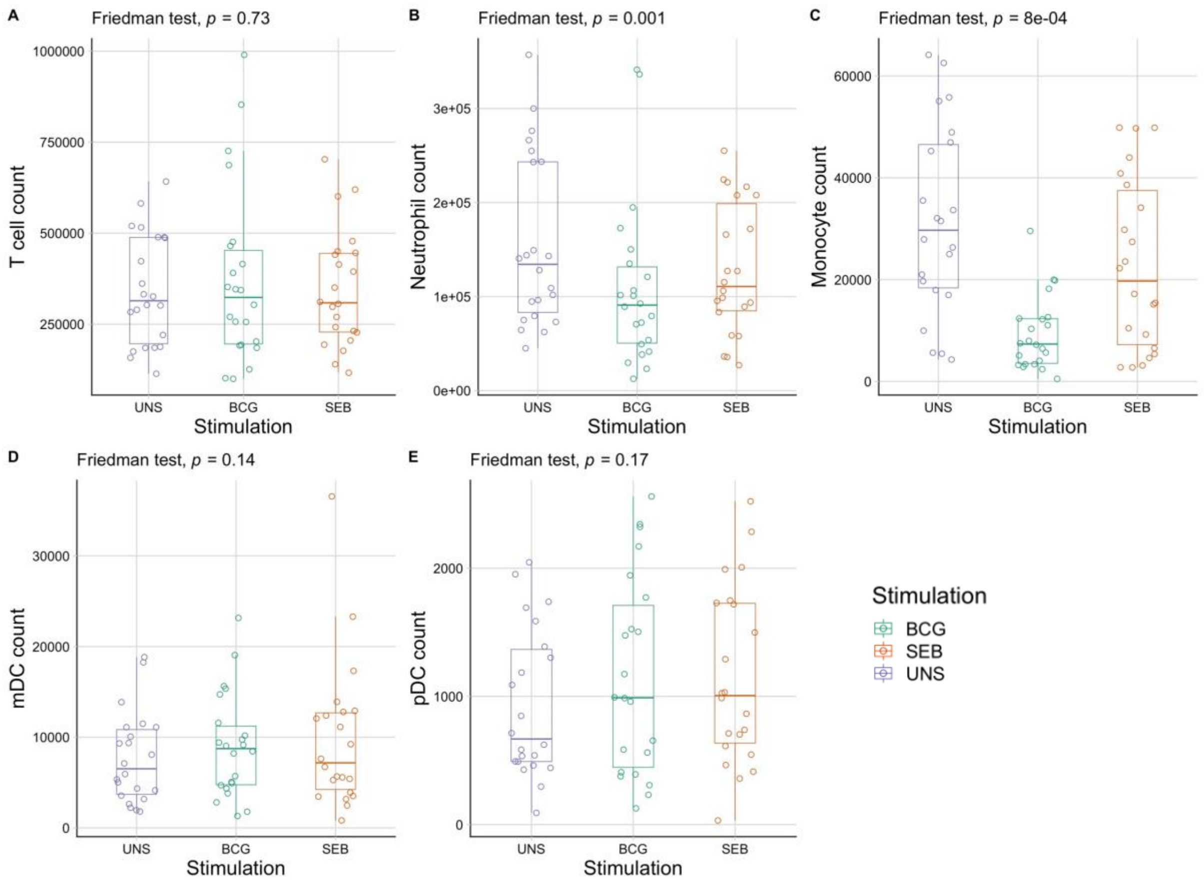

Figure 9. ***Cell counts of cell subsets of interest.*** Boxplots representing the cell counts of **(A)** T cells **(B)** Neutrophils **(C)** Monocytes **(D)** mDCs and **(E)** pDCs across the various stimulations. Horizontal lines represent the median, boxes represent the IQR and whiskers the 95% CI. Differences between cell counts across the various stimulations were calculated with the Friedman test (p<0.05 is significant). Pair-wise comparisons of cell counts between stimulation combinations were calculated using the Wilcoxon signed rank test with Holm-Bonferroni correction for multiple comparisons (p<0.05 was considered significant) (data not visually represented).

T cells

We investigated the pro-inflammatory T cell response to BCG and SEB by measuring IFNγ and TNF expression of CD3+ T cells. BCG has been shown to induce a classical Th1 adaptive immune response with an IFNγ predominance(56). This Th1 response has not been shown to correlate with protection against TB disease(56).

Although the aim of this project primarily is to measure innate responses to BCG, assessing T cell frequencies served as an internal quality control to gauge sample quality and assess whether that sample produced the immune responses for the stimulation conditions it was optimised for. This was important because these samples had been collected and processed over ~20 years ago (**Table A1**). In addition, measuring the overall T cell response allowed us to ensure that the samples reflect T cell cytokine responses in the range that they did when they were first investigated. Lastly, capturing the T cell responses enabled us to investigate correlations between the innate responses and the IFNγ T cell response to BCG(**Fig.15**).

We anticipated that the long period of cryopreservation could potentially reduce the sample quality. In one of the original studies that utilised these samples, a median of 409,077 (IQR, 154,687– 802,636) CD3+ T cells were observed(56). In our study, the medians of CD3+ T cells fall within this range for each of the stimulation conditions (**Fig. 9A**). Exact comparisons between the ranges of cytokine responses to those measured in the original study could not be made as they were assessed separately between CD4+, CD8+ and γδ+ T cells(56). However, T cell expression of IFNγ and TNF was captured by our antibody panel in response to antigen stimulation (**Fig. 10A**) and reflected the range in variability reported in the previous study(56).

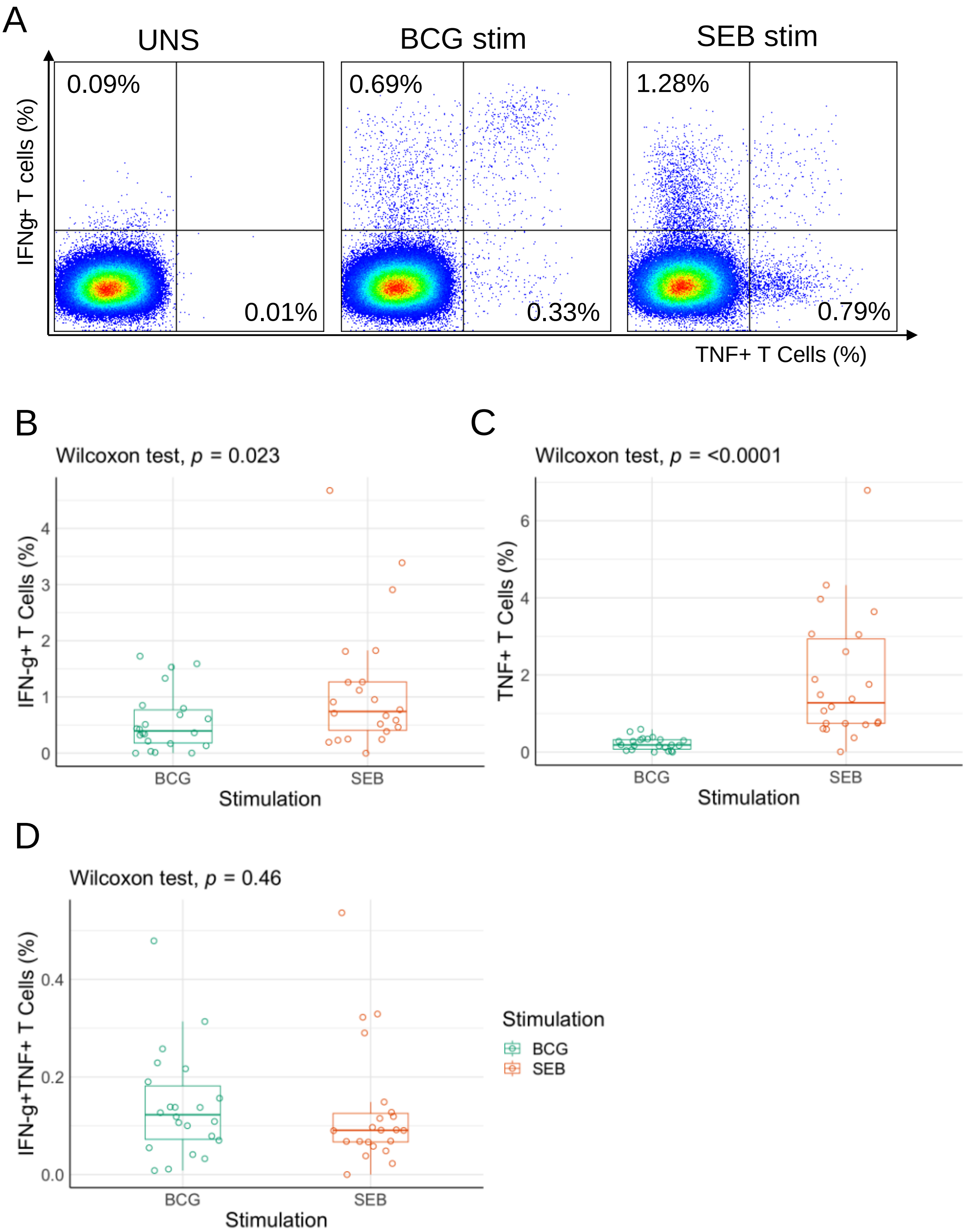

Figure 10. ***T cell cytokine expression.*** **(A)** Representative flow plots of T cell cytokine expression from an infant participant. **(B)** Boxplot representing the frequencies of IFNγ expressing T cells. **(C)** Boxplot representing the frequencies TNF expressing T cells. **(D)** Boxplot representing the frequencies of IFNγ and TNF co-expressing T cells. The cytokine expression data shown from the stimulated samples was background subtracted. Horizontal lines represent the median, boxes represent the IQR and whiskers the 95% CI. Statistical differences of cytokine expression between BCG and SEB stimulated cells were calculated with the Wilcoxon signed rank test ($p<0.05$ was considered significant).

The median frequency of IFNγ expressing T cells in response to BCG was 0.39% (IQR, 0.18% - 0.77%)(**Fig. 10B**), whilst the median frequency in response to SEB was significantly higher at 0.74% (IQR, 0.41% - 1.27%)($p = 0.02$). The median frequency of TNF expressing T cells in response to BCG was 0.19% (IQR, 0.08% - 0.32%) (**Fig. 10C**), whilst the median frequency in response to SEB was significantly higher at 1.28% (IQR, 0.74% - 2.94%)($p = 2.38 \times 10^{-6}$). We also assessed the frequencies of polyfunctional T cells (**Fig. 10D**) and found that the median frequency of IFNγ+TNF+ T cells in response to BCG was 0.12% (IQR, 0.07% - 0.18%) and SEB 0.09% (IQR, 0.07% - 0.13%). The difference between these two was not significant ($p = 0.46$). There was much more variability in IFNγ than TNF expression in response to BCG stimulation whereas the T cell cytokine responses were much variable overall in response to SEB stimulation.

Neutrophils

We then investigated the neutrophil response to BCG or SEB stimulation. Similarly to a previous study from our lab that aimed to study the innate response to BCG, we found that neutrophils were the predominate cell subset in whole blood(**Fig. 9**)(48). We did not assess their ability to express IL-6 like in the original study, as we did not observe any IL-6 responses during the optimisation process (data not shown). However, we were able to capture responses to TNF from these cells (**Fig. 11A**). We found that the median frequency of TNF producing neutrophils was 1.16% (IQR, 0.73% - 2.05%) for BCG and 0.07% (IQR, 0.03% – 0.21%) for SEB stimulated samples, respectively (**Fig. 11B**). The difference between the two was significant ($p = 6.4 \times 10^{-5}$) with higher frequencies of BCG stimulated neutrophils expressing TNF than SEB stimulated neutrophils. The range in variability of TNF responses to BCG stimulation was vast, ranging from 0.00% - 5.21%.

We also observed a huge change in expression of the maturation marker, PD-L1, by neutrophils in response to stimulation (**Fig. 11A**). The overall difference in MFI of PD-L1 across the stimulation conditions were statistically significant ($p = 0.18 \times 10^{-7}$). Pairwise comparisons of MFI between combinations of all three stimulation conditions were also statistically significant (p values < 0.001). This indicates that stimulation with BCG or SEB compared to no stimulation resulted in an increased expression of PD-L1. The median MFI of PD-L1 expression in response to BCG stimulation was 2256 (IQR, 2208 - 3537), whilst the median in response to SEB was higher, at 4044.5 (IQR, 3126 - 5420)(**Fig. 11C**). In contrast to the TNF response, the overall response and variability in PD-L1 expression was much more pronounced in SEB stimulated samples than BCG stimulated samples.

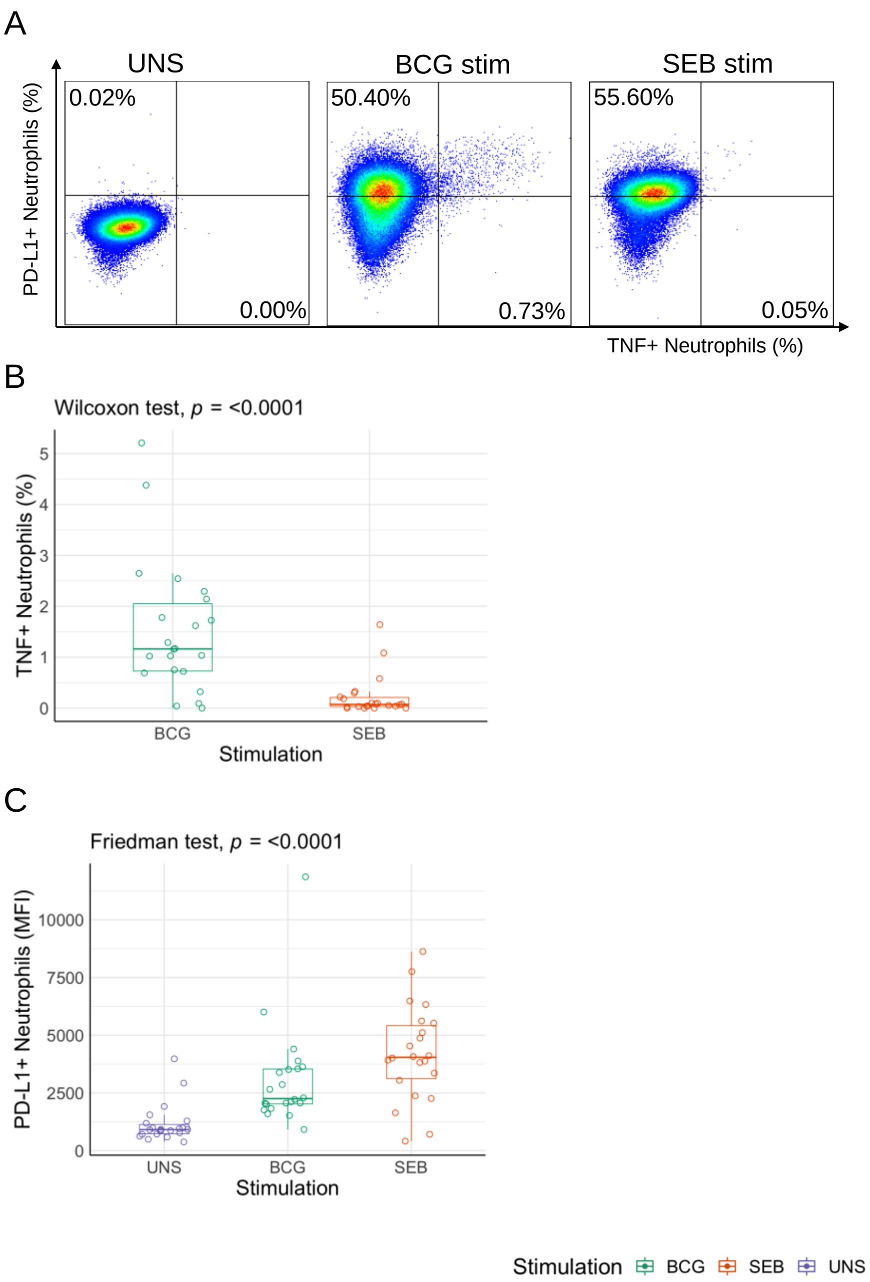

Figure 11. ***Neutrophil cytokine and maturation marker expression.*** **(A)** Representative flow plots of neutrophil cytokine and maturation marker expression from an infant participant. **(B)** Boxplot

representing the frequencies of TNF expressing neutrophils. **(C)** Boxplot representing the MFI of PD-L1 expressing neutrophils. The cytokine expression data shown from the stimulated samples was background subtracted. Horizontal lines represent the median, boxes represent the IQR and whiskers the 95% CI. The individual dots represent individual samples. Statistical differences of cytokine expression between BCG and SEB stimulated cells were calculated with the Wilcoxon signed rank test ($p<0.05$ was considered significant). Differences between MFI across the various stimulations were calculated with the Friedman test. Pair-wise comparisons of MFI between stimulation combinations were calculated using the Wilcoxon signed rank test with Holm-Bonferroni correction for multiple comparisons (data not visually represented).

Myeloid cells – monocytes and mDCs

For monocyte and mDC populations, we assessed both their cytokine and maturation marker expression in response to BCG and SEB stimulation. Although we were measuring cytokine responses from innate cells stimulated for six hours longer than previously optimised in our lab, the assay did capture these responses (**Fig. 12, Fig. 13**). In addition to this, even though stimulation resulted in the down regulation of CD14 expression and affected the number of monocytes we could enumerate(**Fig. 9C**), the assay captured specific cytokine responses and allowed differentiation between monocytes and mDCs (**Fig. 6, Fig.12A, Fig. 13A**).

The median frequency of IL-6-expressing monocytes in response to BCG was 48.92% (IQR, 36.4% - 64.8%) whilst the median frequency in response to SEB was significantly much lower at 0.51% (IQR, 0.11% - 2.18%)($p = 4.76 \times 10^{-7}$) (**Fig. 12B**). The median frequency of TNF expressing monocytes in response to BCG was 10.44% (IQR, 8.11% - 19.8%), whilst the median frequency in response to SEB was also much lower at 0.66% (IQR, 0.19% - 2.16%)($p = 4.47 \times 10^{-4}$) (**Fig. 12C**). Overall, the BCG induced monocytes had larger cytokine responses and showed much more variability in cytokine responses than the SEB induced monocytes. We also assessed the frequencies of polyfunctional monocytes (data not shown), co-expressing IL-6 and TNF. Again, the medians between BCG and SEB induced co-expressing monocytes were significantly different ($p = 3.34 \times 10^{-5}$). A median of 9.14% (IQR, 6.87% - 12.5%) of BCG induced monocytes co-expressed IL-6+TNF+, whereas only 0.03% (IQR, 0% - 0.34%) of SEB induced monocytes did. There was much less variability in responses for monocytes that co-expressed IL-6 and TNF than those that only expressed one cytokine.

The median frequency of IL-6 expressing mDCs in response to BCG was 29.53% (IQR, 23.1% - 42.2%), whilst the median frequency in response to SEB was significantly much lower at 0.30% (IQR, 0.01% - 0.76%)($p = 4.76 \times 10^{-7}$) (**Fig. 13B**). The median frequency of TNF expressing mDCs in response to BCG was 17.6% (IQR, 11.2% - 27.6%), whilst the median frequency in response to SEB was also much lower at 0.80% (IQR, 0.09% - 2.08%)(**Fig. 13C**); again a significant difference ($p = 4.77 \times 10^{-7}$). We also assessed the frequencies of polyfunctional mDCs (data not shown), co-expressing IL-6 and TNF. There was a statistical difference in medians between BCG and SEB induced co-expressing mDCs ($p = 4.77 \times 10^{-7}$). A median frequency of 11.29% (IQR, 8.69% - 21.9%) BCG induced mDCs co-expressed IL-6 and TNF, whereas only 0.07% (IQR, 0% - 0.29%) of SEB induced mDCs did. The overall response and range in variability of cytokine responses in mDCs was much greater for BCG stimulated than SEB stimulated mDCs.

Just as in the case of the neutrophils, we also observed a huge change in expression of the maturation marker, PD-L1 on monocytes and mDCs in response to stimulation (**Fig. 12A, Fig 13A**). The differences in MFI of PD-L1 across the stimulation conditions were significant for both monocytes ($p = 1.29 \times 10^{-7}$) and mDCs ($p= 3.40 \times 10^{-6}$) (**Fig. 12D, Fig 13D**). Pairwise comparisons of MFI of PD-L1 between stimulation conditions were also significant (p values < 0.001); BCG induced monocytes and mDCs had lower PD-L1 MFIs than SEB stimulated cells. The median MFI of PD-L1 expression in response to BCG stimulation for monocytes was 7572 (IQR, 6741 - 10519) whilst as the median in response to SEB was 11915.5 (IQR, 9261 - 16630)($p = 0.003$) (**Fig. 12D**). The median MFI of PD-L1 expression in response to BCG stimulation for mDCs was 7843 (IQR, 5848 - 10126) whilst as the median in response to SEB was 10101 (IQR, 7406 - 13822)($p = 0.043$) (**Fig. 13D**). The range in variability of responses for SEB induced monocytes and mDCs was much higher than the range of BCG induced cells. However, the variability in the BCG response appeared suitable to identify associations with SNPs.

Lastly, we also assessed the expression of CD40 on monocytes and mDCs in response to stimulation. The overall differences in MFI of CD40 across the stimulation conditions relative to the unstimulated condition were statistically significant for both monocytes and mDCs ($p = <0.0001$). (**Fig. 12E, Fig 13E**). The median MFI of CD40 expression in response to BCG stimulation for monocytes was 1208 (IQR, 848 - 1504) whilst the median in response to SEB was 1331 (IQR, 980 - 1707)(**Fig. 12E**). The median MFI of CD40 expression in response to BCG stimulation for mDCs was 1446 (IQR, 915 - 1707) whilst the median in response to SEB was 1553.5 (IQR, 929 - 1738)(**Fig. 13E**). Pairwise comparisons of the MFI of CD40 between BCG and SEB stimulation conditions was significant for monocytes (SEB higher, $p = 0.02$), however, this was not significant for mDCs ($p = 0.824$). Overall, both the response and variability in CD40 responses for SEB stimulated monocytes and mDCs was higher than the BCG stimulated cells but the difference was small.

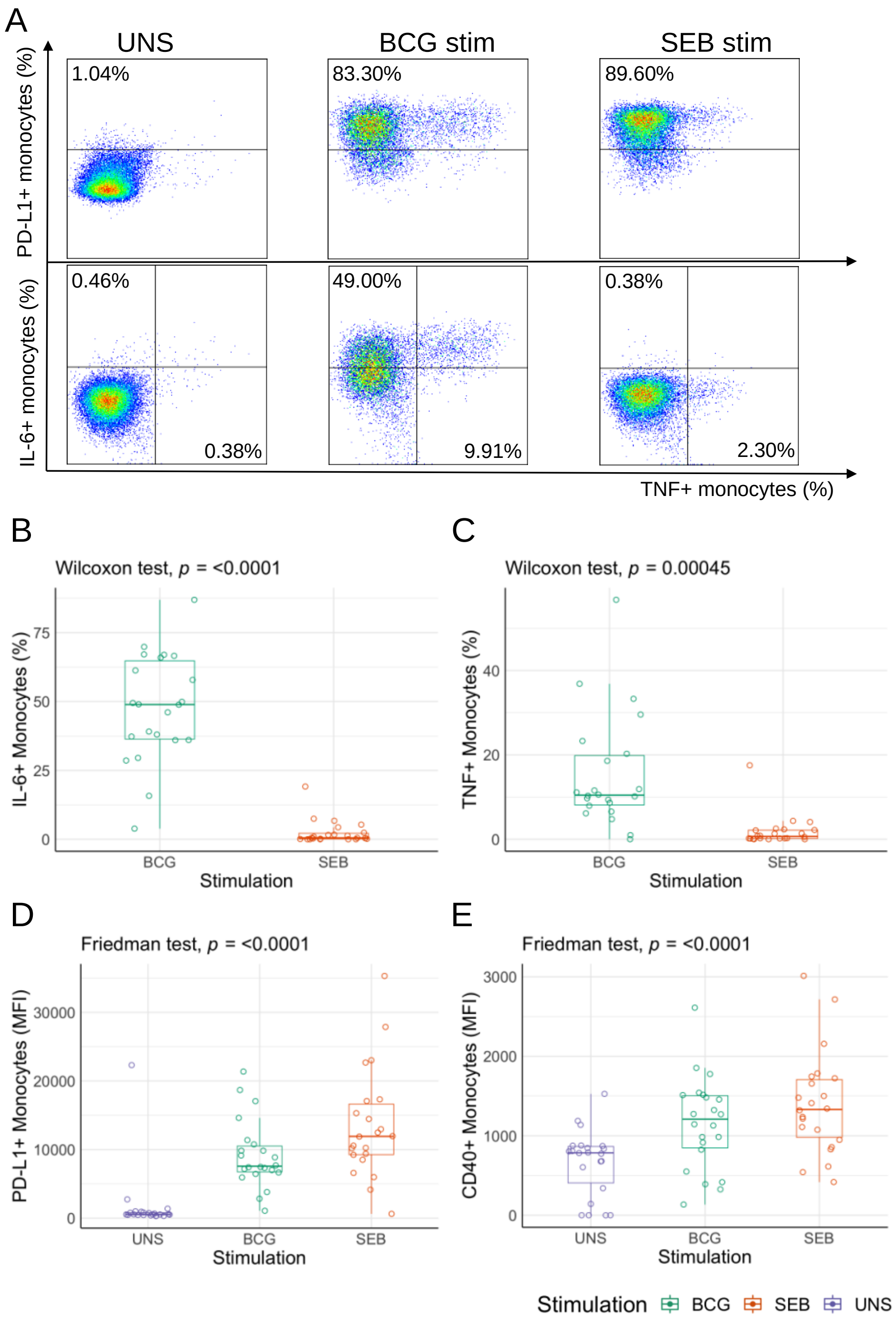

Figure 12. ***Monocyte cytokine and maturation marker expression.*** **(A)** Representative flow plots of monocyte cytokine and maturation marker expression from an infant participant. **(B)** Boxplot representing the frequencies of IL-6 expressing monocytes. **(C)** Boxplot representing the frequencies TNF expressing monocytes. **(D)** Boxplot representing the MFI of PD-L1 expressing monocytes. **(E)** Boxplot representing the MFI of CD40 expressing monocytes. The cytokine expression data shown from the stimulated samples was background subtracted. Horizontal lines represent the median, boxes represent the IQR and whiskers the 95% CI.Differences of cytokine expression between BCG and SEB stimulated cells were calculated with the Wilcoxon signed rank test ($p<0.05$ is significant). Differences between MFI across the various stimulations were calculated with the Friedman test

(p<0.05 is significant). Pair-wise comparisons of MFI between stimulation combinations were calculated using the Wilcoxon signed rank test with Holm-Bonferroni correction for multiple comparisons (p<0.05 was considered significant) (data not visually represented).

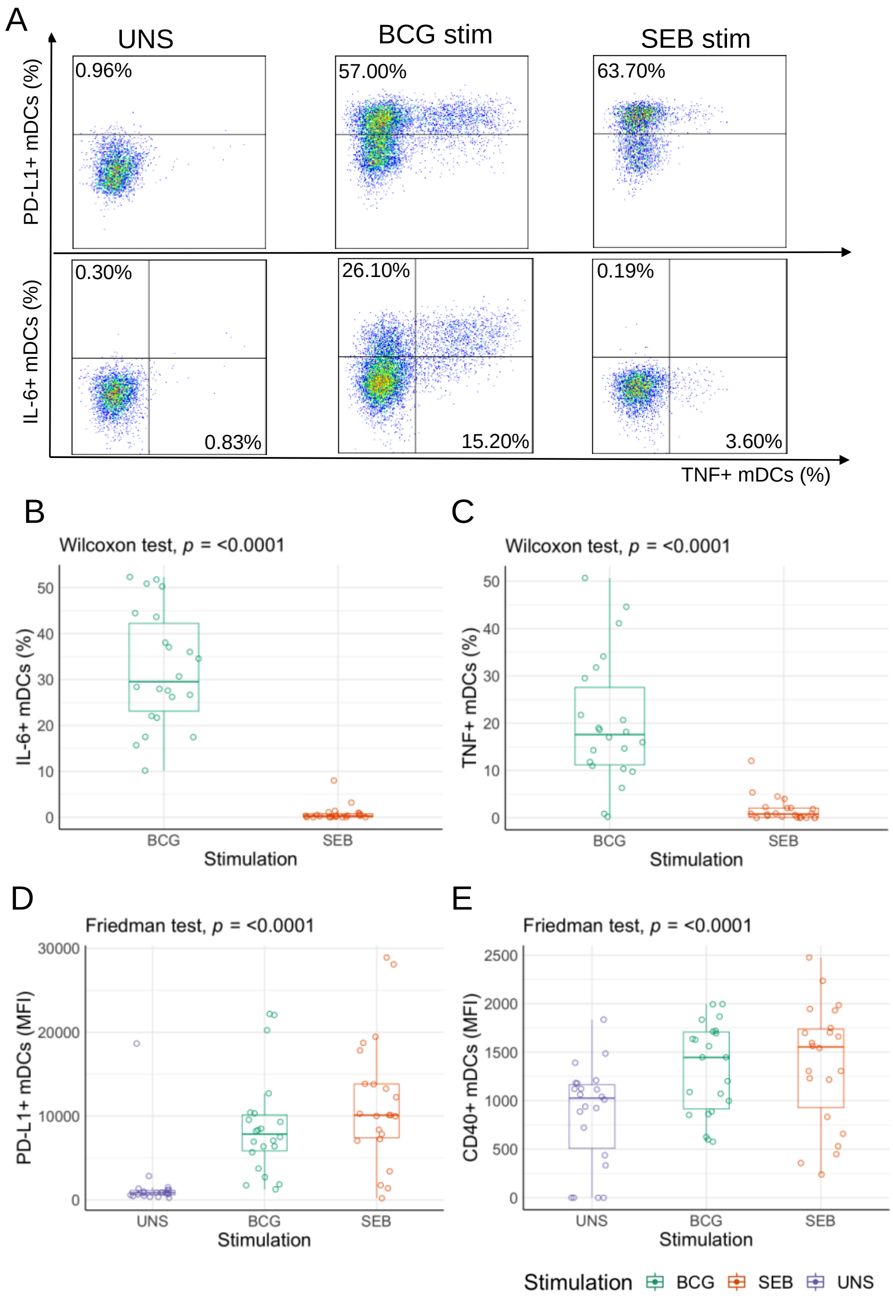

Figure 13. ***Myeloid dendritic cell cytokine and maturation marker expression.*** **(A)** Representative flow plots of mDC cytokine and maturation marker expression from an infant participant. **(B)** Boxplot representing the frequencies of IL-6 expressing mDCs. **(C)** Boxplot representing the frequencies TNF expressing mDCs. **(D)** Boxplot representing the MFI of PD-L1 expressing mDCs. **(E)** Boxplot representing the MFI of CD40 expressing mDCs. The cytokine expression data shown from the

stimulated samples was background subtracted. Horizontal lines represent the median, boxes represent the IQR and whiskers the 95% CI. Statistical differences of cytokine expression between BCG and SEB stimulated cells were calculated with the Wilcoxon signed rank test ($p<0.05$ is significant). Differences between MFI across the various stimulations were calculated with the Friedman test ($p<0.05$ is significant). Pair-wise comparisons of MFI between stimulation combinations were calculated using the Wilcoxon signed rank test with Holm-Bonferroni correction for multiple comparisons ($p<0.05$ is significant) (data not visually represented).

pDCs

Lastly, we assessed the expression of cell maturation markers to pDCs in response to BCG and SEB stimulation (**Fig. 14**). Relatively to the unstimulated samples, both BCG and SEB stimulation increased the expression of both PD-L1 and CD40 of pDCs (**Fig. 14A, Fig. 14B**).

The overall difference in MFI of CD40 across the stimulation conditions were statistically significant ($p = 2.33 \times 10^{-8}$). Pairwise comparisons of MFI of CD40 between combinations of all three stimulation conditions were also statistically significant (p values < 0.001). The median MFI of CD40 expression in response to BCG stimulation was 646.5 (IQR, 592 - 813) whereas the median in response to SEB was much higher at 1184.5 (IQR, 854 - 1569)($p = 1.31 \times 10^{-4}$)(**Fig. 14C**). There was more variability in responses in CD40 expression by pDCs to SEB stimulation than BCG stimulation. However, the variability in the BCG response is acceptable to conduct downstream genetic analysis.

The overall difference in MFI of PD-L1 across the stimulation conditions were also statistically significant ($p = 1.29 \times 10^{-8}$). Pairwise comparisons of MFI of PD-L1 between combinations of all three stimulation conditions were also statistically significant (p values < 0.001). The median MFI of PD-L1 expression in response to BCG stimulation was 702 (IQR, 498 - 792) whilst as the median in response to SEB was 1776.5 (IQR, 718 - 3318) ($p = 2.42 \times 10^{-4}$)(**Fig. 14D**). There was limited variability in PD-L1 responses by pDCs to BCG responses but in contrast, there was a vast variability in the range of responses to SEB stimulation.

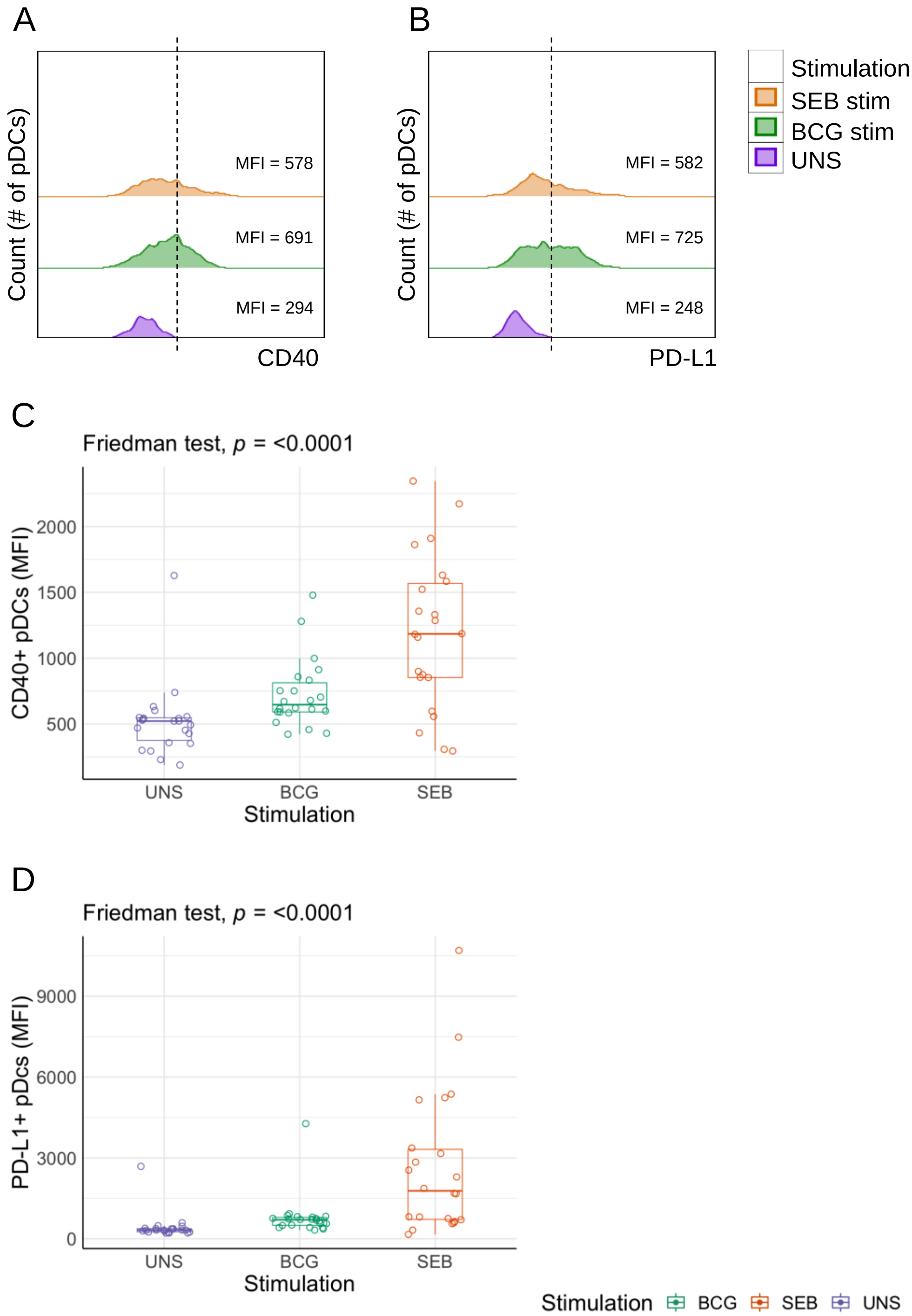

Figure 14. ***Plasmacytoid dendritic cell maturation marker expression.*** **(A)** Representative offset histogram plots of CD40 expression from an infant participant. **(B)** Representative offset histogram plots of PD-L1 expression from an infant participant. A unimodal shift in fluorescence is observed in response to stimulation (dotted line). Numbers represent the median fluorescence intensity (MFI) for each marker for each stimulation condition. **(C)** Boxplot representing the MFI of CD40 expressing monocytes. **(D)** Boxplot representing the MFI of PD-L1 expressing monocytes. Horizontal lines represent the median, boxes represent the IQR and whiskers the 95% CI. Differences between MFI across the various stimulations were calculated with the Friedman test ($p<0.05$ is significant). Pair-

wise comparisons of MFI between stimulation combinations were calculated using the Wilcoxon signed rank test with Holm-Bonferroni correction for multiple comparisons ($p<0.05$ is significant) (data not visually represented).

Correlation between IFNg expressing T cells and maturation marker expression of innate cells

Finally, in line with the larger aims of this project, we investigated the relationship between the IFNγ T cell response to BCG or SEB stimulation and the cell maturation marker expression of the various innate cells of interest. This was informed by our hypothesis that IFNγ expression by T cells may induce upregulation of PD-L1 or CD40 by innate cells. We assessed this by correlating the frequency of IFNγ+ CD3+ T cells to the MFI of either PD-L1 or CD40 of our innate cells of interest in response to stimulation (**Fig.15**).

Overall, no correlations between the frequency of IFNγ expressing CD3+ T cells and the cell maturation marker expression of neutrophils and monocytes for either stimulation condition were observed (**Fig 15. A, B, C**). CD40 expression and T cell IFNγ expression by mDCs were also not correlated (**Fig. 15D**). However, BCG-induced mDC expression of PD-L1 was moderately correlated with T cell IFNγ expression ($R = 0.44$, $p = 0.04$) (**Fig 15E**). Lastly, stronger associations for pDCs between maturation marker and IFNγ expression for both stimulation conditions were observed. There was a statistically significant, moderate, positive correlation between IFNγ+ T cells and the expression of CD40 on BCG ($R = 0.46$, $p = 0.032$) and SEB ($R = 0.43$, $p = 0.048$) stimulated pDCs (**Fig. 15F**). A moderate positive correlation between IFNγ+ T cells and the expression of PD-L1 on BCG ($R = 0.41$, $p = 0.061$) and SEB ($R = 0.47$, $p = 0.028$) stimulated pDCs was observed (**Fig. 15G**).

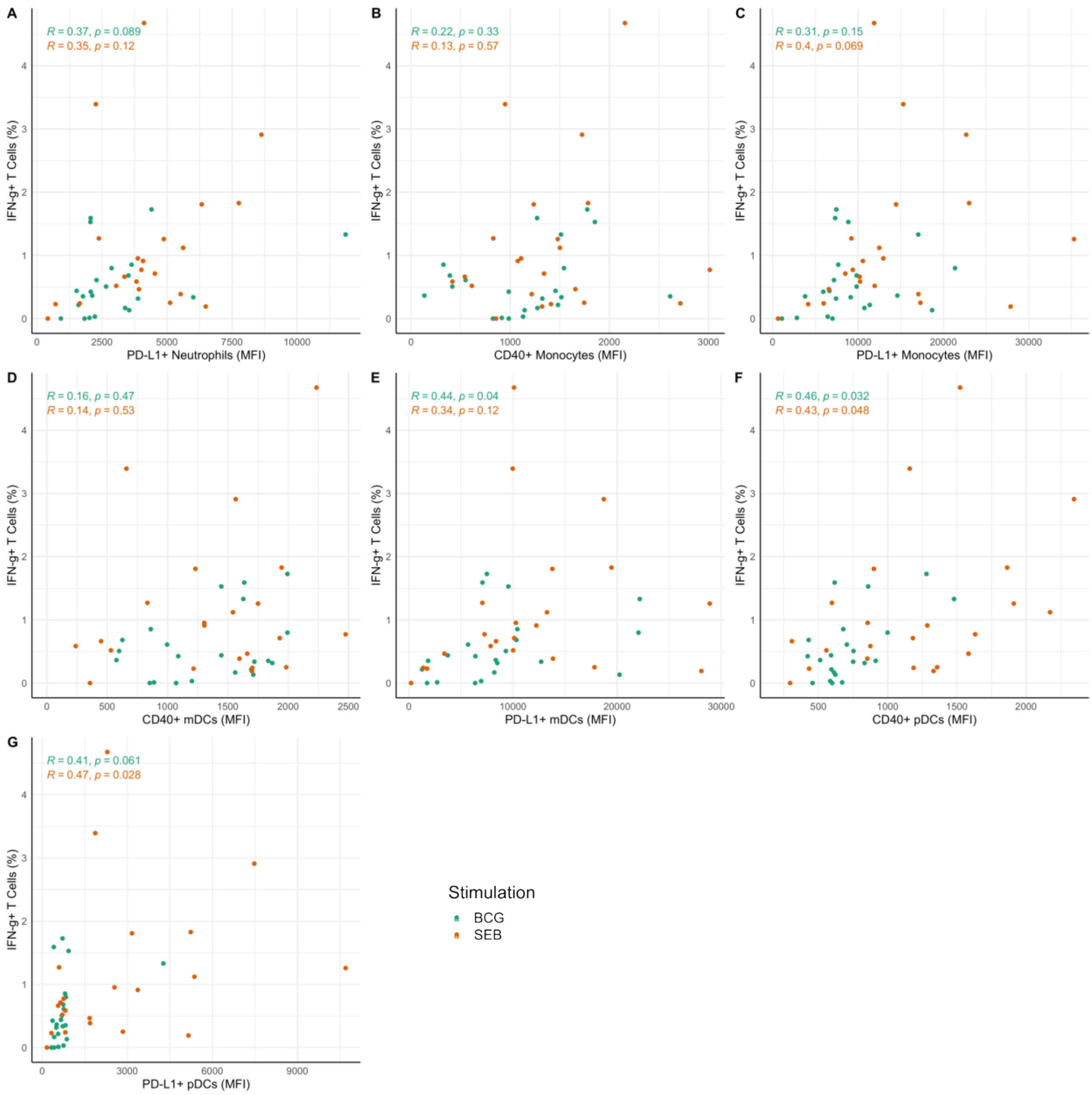

Figure 15. ***Correlation between IFNγ expressing T Cells and maturation marker expression of innate cells.*** Correlation graphs between frequency of IFNγ expressing T cells and the MFI of **(A)** PD-L1+ neutrophils, **(B)** CD40+ monocytes, **(C)** PD-L1+ monocytes, **(D)** CD40+ mDCs, **(E)** PD-L1+ mDCs , **(F)** CD40+ pDCs, **(G)** PD-L1+ mDCs. The cytokine expression data shown from the stimulated samples was background subtracted. The degree of correlation was measured using Spearman's correlation coefficient($p<0.05$ is significant).

Discussion

The main objective of this chapter was to report the range in functional responses by innate cells in 25 BCG vaccinated, ten-week-old infants. We aimed to estimate the variability in the BCG innate response as a proof-of-concept to assess whether the dynamic range in response outcomes would be sufficient to enable our collaborators to identify SNPs associated with innate responses to BCG. Specifically, we measured the expression of pro-inflammatory cytokines IL-6 and TNF and the maturation markers CD40 and PD-L1 in neutrophils, monocytes, mDCs and pDCs. Additionally, we measured the T cell IFNγ and TNF response to BCG and correlated this with the cell maturation marker expression of the various innate cells of interest.

This chapter reported on the innate responses of 25 out of the 200 participants that will be analysed for the larger project. We excluded three participants in the final analysis in accordance with the visual flow cytometric quality control criteria we established. These samples were assessed to be of poor quality and thus, this chapter describes data for 22 infant participants. By assessing T cell frequencies and the T cell response, we were able to ensure that the samples produced the immune responses for the stimulation conditions it was optimised for and reflected T cell cytokine responses in the range similar to prior studies(56). This was important given the age of the samples.

Exact comparisons between the range of cytokine responses to those measured in the original study could not be made as they were assessed separately between CD4+, CD8+ and γδ+ T cells(56). However, IFNγ and TNF T cell expression was captured by our antibody panel in response to antigen stimulation. The T cell response to BCG was predominantly mediated by IFNγ. The IFNγ T cell cytokine response showed much greater variability in responses than the TNF cytokine response in response to BCG stimulation. This is unsurprising because T cells are known to have an IFNγ dominant response to mycobacteria and our lab and others have previously shown IFNγ+ T cells to be the majority subset of cells(11, 56). There was much greater response and variation in TNF responses to SEB stimulation than BCG responses.

Despite the six hours longer stimulation duration and different BCG concentration used for our samples previously optimised for innate studies, we were still able to successfully capture the innate responses of the 22 infant participants and estimate the variability in responses to BCG and SEB stimulation using our flow cytometry panel. The range in magnitude of IL-6 responses for monocytes and mDCs, for example, was comparable to those found by Shey et al(48). We were also able to successfully capture TNF responses from neutrophils which was not observed by the 6-hour innate response assay previously optimised(48). However, we were also not able to capture significant IL- 6 responses by neutrophils and therefore omitted pursuing this analysis(48). Lastly, using MFI we were also able to successfully assess changes in expression for the maturation markers, CD40 and PD-L1, for neutrophils, monocytes, mDCs and pDCs and subsequently correlate these changes with IFNγ expression by T cells. Our ability to capture these various responses by flow cytometry reinforces that our 13-colour flow cytometry panel was well optimised to measure innate immune responses for the stimulation conditions of our infant samples.

Eum et al demonstrated that neutrophils are the most abundant cell type in both sputum and bronchoalveolar lavage samples of active TB patients; these cells were also most infected with *M. tb* and contained more *M. tb* compared to macrophages(23). *M. tb* is known to stimulate neutrophils to secrete TNF, which helps to recruit and activate other immune cells and enhance macrophage killing(13). We found a low range of TNF expression in response to BCG stimulation that would likely still be amenable to correlating with genetic analysis to find polymorphisms that may help us understand the role of this in the context of BCG vaccination. In contrast, we did not observe such a vast range in PD-L1 expression by BCG induced neutrophils. Conversely to the BCG response, we found a very small TNF response to SEB but a larger and more variable response to PD-L1 by SEB induced neutrophils. In a study that compared active TB patients with healthy controls, it was found that PD-L1 was highly expressed in whole blood, and this was largely driven by expression on neutrophils(51). The PD1/PD-L1 immunoregulatory pathway supresses T cell receptor activation and T cell IFNγ production and immune cytotoxicity and suppresses protective immunity in TB disease in order to prevent severe TB immunopathology(51). Utilising genome wide approaches may uncover the role of this immunoregulatory paradigm in the context of BCG vaccination.

In response to BCG stimulation, IL-6 was the more abundant cytokine expressed by both monocytes and mDCs than TNF, with a greater proportion of monocytes expressing IL-6 than mDCs. This was also observed in the 6-hour innate assay optimised by Shey et al(48). Our lab and collaborators have previously shown that altered IL-6 secretion in stimulated whole blood was associated two polymorphisms in an adult population and that Toll-interacting protein deficient monocytes had increased IL-6 expression(61, 62). The variability of IL-6 responses by monocytes and mDCs in response to BCG by previously vaccinated infants in our study potentially lends itself to identification of more SNPs associated with variability in BCG-induced IL-6 responses.

We observed that a larger proportion of mDCs expressed TNF overall and co-expressed TNF and IL-6 in response to BCG stimulation than monocytes. Although we did not observe that TNF and IL-6 co-expressing cells were the most dominant mDC subset like Shey et al, we also observed that mDCs had a higher proportion of co-expressing cells than monocytes. This further supports that the differentiation between monocytes and mDCs was reasonable despite challenges in separating the two populations. We observed a much greater IL-6 and TNF cytokine response to BCG stimulation than SEB stimulation by monocytes and mDCs. This is why SEB was a more appropriate positive control for the T cell assay whereas LPS is more appropriate for innate assays.

We included the maturation markers CD40 and PD-L1 in our panel in line with the work of our collaborators. Using a murine model, our collaborators used a genome-wide knockout screen in order to elucidate the genes important for regulating expression of co-stimulatory markers on myeloid cells, their response to IFNγ, as well as their ability to prime T cell IFNγ expression. Stimulation of BMDMs with IFNγ upregulated the expression of the co-stimulatory markers MHC II, CD40 and PD-L1(59). Using a CRISPR-Cas9 screen, they were then able to identify the genes that were upregulated in response to expression of these markers and implicate complex

I of the electron transport chain as a key regulator of IFNγ-mediated gene expression in BMDMs(59). By assessing CD40 and PD-L1 expression in response to BCG vaccination in infants we sought to measure a range in magnitude of responses to ultimately identify polymorphisms that were associated with these responses in the regulatory genes that our collaborators found.

We observed that stimulation with BCG or SEB resulted in significant changes in expression maturation markers CD40 and PD-L1 for monocytes, mDCs and pDCs**.** Overall, we observed that SEB stimulated samples had much higher and more variable changes in CD40 and PD-L1 expression compared to BCG stimulated samples, particularly for the pDCs. This contrasted with the cytokine responses. The innate cells had minimal cytokine responses to SEB but had much larger changes in expression of the maturation markers upon stimulation. In the 6-hour innate assay previously optimised by our lab, changes in expression to CD40 by monocytes and mDCs in response to BCG were also measured by MFI (unpublished data). The range in magnitude of CD40 responses for BCG-induced monocytes and mDCs were comparable to those previously found by our lab (unpublished data). This is reassuring as it further confirms that our panel was able to reliably measure innate responses to BCG despite the different stimulation durations.

Lastly, we investigated the relationship between the IFNγ T cell response to BCG or SEB stimulation and the cell maturation marker expression of the various innate cells of interest. We assessed this by determining which innate outcomes correlated with frequencies of IFNγ+ CD3+ T cells. Overall, we found no strong correlations between the frequency of IFNγ expressing CD3+ T cells and the cell maturation marker expression of the innate cells of interest. Curiously, we observed moderate, positive correlations between T cell IFNg expression and mDC PD-L1 expression as well as pDC CD40 and PD-L1 expression in response to both BCG and SEB stimulation. These associations should be further explored in the larger subset of 200 infants. BCG has been shown to modulate pDCs to promote their ability to induce regulatory T cells *in vitro*(63). The immune regulatory role of pDCs in the context of BCG vaccination or *M. tb* infection is poorly understood. By using a similar genome-wide knockout screen approach our collaborators used, eliciting the genes important for regulating expression of co-stimulatory markers on pDCS in the context BCG vaccination may be achieved.

A major limitation of this project is that we were not able to adequately separate the monocyte and mDC populations with our panel because of poor CD14 resolution. Reduction of CD14 is thought to be likely due to shedding of CD14 or monocyte death upon stimulation as monocytes are known to rapidly die after phagocytosis of mycobacteria(48). In the 6-hour innate assay previously optimised by our lab, it was noted that incubation of whole blood with BCG resulted in detection of markedly lower frequencies of CD14+ monocytes and therefore recommendations were made for the optimisation of staining conditions to better detect monocytes(48). Thus, we anticipated to encounter this challenge and attempted to improve detection of monocytes with the inclusion of a second myeloid lineage marker, CD33, in our panel. CD33 was less downregulated in response to stimulation and therefore aided in the identification of the myeloid cells of interest. However, it was still challenging to adequately separate the monocyte and mDC populations, particularly for the BCG stimulated samples. Although we are confident that we were able to estimate the variability in immune responses for monocytes and mDCs and that this can be applied to the larger 200 infant cohort, this lack of certainty in distinction between these myeloid cells makes it harder to truly assign immune outcomes we measured to monocytes and mDC. In light of this uncertainty it may be best to report these outcomes for CD33+ myeloid cells (i.e. monocytes and mDC combined).

Although a sample size of 25 participants was adequate to allow an estimation of the immune response outcomes, an even larger sample size would have enabled us to more accurately assess the correlations between innate responses and IFNγ T cell responses. This limitation of sample size may be addressed in the overall sample size of 200 participants in the larger project. We were limited by the number of immune response outcomes we measured due to the size of our antibody panel due to the cost of antibodies and flow cytometer capacity but, for example, we would have benefited from measuring IL-12 or IL-10 responses. Estimating the variability in the range of these responses is a missed opportunity particularly as the data generated in this study will potentially be correlated with genetic analysis that may uncover SNPs in other immune responses also shown to be key in the modulation of the BCG immune response. Additionally, this study could have benefited from assessing BCG induced responses in other innate cell types such as NK cells.

In conclusion, a 13-colour flow cytometry antibody panel was successfully optimised for enumerating and measuring cytokine and cell maturation marker expression by neutrophils, monocytes, mDCs, pDCs, and T cells in response to BCG stimulation. Expression of cytokines (IFNγ, IL-6, TNF) and maturation markers (CD40, PD-L1) by these cell subsets to BCG stimulation were quantified, allowing identification of single nucleotide polymorphisms that associate with variability in innate responses to BCG. Overall, we observed a large range in variability in immune responses from innate cells to BCG stimulation among the 22 infants that supports studies to identify genetic association with innate response outcomes. Results from this MSc thus inform the bigger project which aims to determine genetic determinants of innate responses to BCG and TB disease risk. In fact, the optimised flow cytometry antibody panel has been applied to measure these outcomes in the larger set of 200 infant samples. To this end, this work has enabled a more comprehensive study that aims to identify the genetic factors that result in variable infant innate responses to BCG vaccination and in so doing expand the basis of learning for novel TB vaccine candidates.

References

1. World Health Organization. 2022. Global Tuberculosis report 2022. WHO Publishing Group.

2. Behr MA, Kaufmann E, Duffin J, Edelstein PH, Ramakrishnan L. 2021. Latent Tuberculosis: Two centuries of confusion. Am J Respir Crit Care Med 204(2):142-148.

3. Jain A, Mondal R. 2008. Extensively drug-resistant Tuberculosis: Current challenges and threats. FEMS Immunol Med Microbiol 53:145–150.

4. World Health Organization. 2020. WHO report on TB 2020. WHO Publishing Group.

5. Perrin P. 2015. Human and Tuberculosis co-evolution: An integrative view. Tuberculosis 95: S112–S116.

6. Sanou A, Bañuls A-L, van Anh NT, Godreuil S. 2015. *Mycobacterium tuberculosis*: ecology and evolution of a human bacterium. J Med Microbiol 64:1261–1269.

7. Woo M, Wood C, Kwon D, Park K-HP, Fejer G, Delorme V. 2018. *Mycobacterium tuberculosis* infection and innate responses in a new model of lung alveolar macrophages. Front Immunol 9:1–13.

8. Zager EM, McNerney R. 2008. Multidrug-resistant tuberculosis. BMC Infect Dis 8:1–5.

9. Amaral EP, Lasunskaia EB, D’Império-Lima MR. 2016. Innate immunity in tuberculosis. How the sensing of *mycobacteria* and tissue damage modulates macrophage death. Microbes Infect 18:11–20.

10. Liu CH, Liu H, Ge B. 2017. Innate immunity in tuberculosis: host defence vs pathogen evasion. Cellular & Molecular Immunology 14:963.

11. Ernst JD. 2012. The immunological life cycle of tuberculosis. Nat Rev Immunol 12.

12. Tenland E, Håkansson G, Alaridah N, Lutay N, Rönnholm A, Hallgren O, Westergren-Thorsson G, Godaly G. 2016. Innate immune responses after airway epithelial stimulation with *Mycobacterium bovis Bacille-Calmette Guérin*. PLoS One 11:1–15.

13. Gupta N, Kumar R, Agrawal B. 2018. New players in immunity to tuberculosis: The host microbiome, lung epithelium, and innate immune cells. Front Immunol 9:1–10.

14. Reuschl A-K, Edwards MR, Parker R, Connell DW, Hoang L, Halliday A, Jarvis H, Siddiqui N, Wright C, Bremang S, Newton SM, Beverley P, Shattock RJ, Kon OM, Lalvani A. 2017. Innate activation of human primary epithelial cells broadens the host response to *Mycobacterium tuberculosis* in the airways. PLoS Pathog 13: e1006577.

15. Cywes L, Hoppe HC, Daffé M, Ehlers MRW. 1997. Nonopsonic binding of *Mycobacterium tuberculosis* to complement receptor type 3 is mediated by capsular polysaccharides and is strain dependent. Infect Immune 65:4258–4266.

16. Roberts EA, Deretic V. 2008. The *Mycobacterium tuberculosis* phagosome, p. 439–449. *In* Deretic, V (ed.), autophagosome and phagosome. Humana Press, Totowa, NJ.

17. Awuh JA, Flo TH. 2017. Molecular basis of *mycobacterial* survival in macrophages. Cell Mol Life Sci 74:1625–1648.

18. Weiss G, Schaible UE. 2015. Macrophage defence mechanisms against intracellular bacteria. Immunol Rev 264:182–203.

19. Zhang YJ, Reddy MC, Ioerger TR, Rothchild AC, Schuster BM, Trauner A, Wallis D, Galaviz S, Sacchettini JC, Behar SM, Rubin EJ. 2014. Tryptophan biosynthesis protects *mycobacteria* from CD4 T-cell-mediated killing. Cell 155:1296–1308.

20. Parish T. 2003. Starvation survival response of *Mycobacterium tuberculosis*. J Bacterial 185:6702–6.

21. Yang R, Yang E, Shen L, Modlin RL, Shen H, Chen ZW. 2018. IL-12+IL-18 Cosignaling in human macrophages and lung epithelial cells activates cathelicidin and autophagy, inhibiting intracellular *mycobacterial* growth. J Immunol 200(7):2405-2417.

22. Keane J, Remold HG, Kornfeld H. 2000. Virulent mycobacterium tuberculosis strains evade apoptosis of infected alveolar macrophages. J Immunol 164:2016–2020.

23. Eum SY, Kong JH, Hong MS, Lee YJ, Kim JH, Hwang SH, Cho SN, Via LE, Barry CE. 2010. Neutrophils are the predominant infected phagocytic cells in the airways of patients with active pulmonary TB. Chest 137:122–128.

24. Tan BH, Meinken C, Bastian M, Bruns H, Legaspi A, Ochoa MT, Krutzik SR, Bloom BR, Ganz T, Modlin RL, Stenger S. 2006. Macrophages acquire neutrophil granules for antimicrobial activity against intracellular pathogens. J Immunol 177:1864–1871.

25. Sampath P, Moideen K, Ranganathan UD, Bethunaickan R. 2018. Monocyte subsets: phenotypes and function in tuberculosis infection. Front Immunol 9:1726.

26. Scriba TJ, Coussens AK, Fletcher HA. 2017. Human immunology of tuberculosis. Microbiol Spectr 5(1).

27. Kim H, Shin SJ. 2022. Pathological and protective roles of dendritic cells in *Mycobacterium tuberculosis* infection: Interaction between host immune responses and pathogen evasion. Front Cell Infect Microbiol 12:891878.

28. Lozza L, Farinacci M, Bechtle M, Stäber M, Zedler U, Baiocchini A, del Nonno F, Kaufmann SHE. 2014. Communication between human dendritic cell subsets in tuberculosis: requirements for naive CD4+ T cell stimulation. Front Immunol 5.

29. O'Garra A, Redford PS, McNab FW, Bloom CI, Wilkinson RJ, Berry MPR. 2013. The immune response in tuberculosis. Annu Rev Immunol 31:475-527.

30. Arko-Mensah J, Julián E, Singh M, Fernández C. 2007. TLR2 but not TLR4 signalling is critically involved in the inhibition of IFN-γ-induced killing of *mycobacteria* by murine macrophages. Scand J Immunol 65:148–157.

31. Cambier CJ, Falkow S, Ramakrishnan L. 2014. Host evasion and exploitation schemes of *Mycobacterium tuberculosis*. Cell 159:1497–1509.

32. Martin C, Aguilo N, Gonzalo-asensio J. 2018. Vaccination against tuberculosis. Enferm Infecc Microbiol Clin 36:648–656.

33. Dockrell HM, Smith SG. 2017. What have we learnt about BCG vaccination in the last 20 years? Front Immunol 8:1–10.

34. Moliva JI, Turner J, Torrelles JB. 2017. Immune responses to bacillus Calmette-Guérin vaccination: Why do they fail to protect against *Mycobacterium tuberculosis*? Front Immunol 8:407.

35. Butkeviciute E, Jones CE, Smith SG. 2018. Heterologous effects of infant BCG vaccination: potential mechanisms of immunity. Future Microbiol 13:1193–1208.

36. Dowd JB, Fletcher HA, Boccia D. 2018. Social determinants and BCG efficacy: a call for a socio-biological approach to TB prevention. F1000Res 7:224.

37. Smith CM, Proulx MK, Olive AJ, Laddy D, Mishra BB, Moss C, Gutierrez NM, Bellerose MM, Barreira-silva P, Phuah Y, Baker RE, Behar SM. 2016. Tuberculosis susceptibility and vaccine protection are independently controlled by host. Genotype 7:1–13.

38. Casanova J, Abel L. 2002. Genetic dissection to immunity to mycobacteria: The human model. Annu Rev Immunol 581–620.

39. Naranbhai V. 2016. The Role of host genetics (and genomics) in tuberculosis. Microbiol Spectr 4(5).

40. Casanova J, Holland SM, Notarangelo LD. 2012. Review inborn errors of human JAKs and STATs. Immunity 21:515–528.

41. Abu Toamih Atamni H, Nashef A, Iraqi FA. 2018. The collaborative cross mouse model for dissecting genetic susceptibility to infectious diseases. Mamm Genome 29:471–487.

42. Hawkridge A, Hatherill M, Little F, Goetz MA, Barker L, Mahomed H, Sadoff J, Hanekom W, Geiter L, Hussey G, Burger A, Malone A, Demers AM, Veldsman A, Gumusboga A, Kewley C, Minnies D, Michaels D, Simon E, Kaplan G, Zar H, Iloni K, Denation L, Workman L, van der Merwe L, Behr M, Buchanan M, Borgdorff M, Geldenhuys M, Kibel M, Tameris M, Hanslo M, Shepherd R, Schaaf S, Mawu S, Moyo S, Abraham S, Verver S, Mlanjeni S, Dirks V. 2008. Efficacy of percutaneous versus intradermal BCG in the prevention of tuberculosis in South African infants: Randomised trial. BMJ 337:1275–1278.

43. Hanekom WA, Hughes J, Mavinkurve M, Mendillo M, Watkins M, Gamieldien H, Gelderbloem SJ, Sidibana M, Mansoor N, Davids V, Murray RA, Hawkridge A, Haslett PAJ, Ress S, Hussey GD, Kaplan G. 2004. Novel application of a whole blood intracellular cytokine detection assay to quantitate specific T-cell frequency in field studies. J Immunol Methods 291:185–195.

44. Villas BH. 1998. Flow cytometry: an overview. Cell Vis 5:56–61.

45. Mahnke YD, Roederer M. 2007. Optimizing a multicolour immunophenotyping assay. Clin Lab Med 27:469–485.

46. Perfetto SP, Chattopadhyay PK, Roederer M. 2004. Seventeen-colour flow cytometry: unravelling the immune system. Nat Rev Immunol 4:648–655.

47. Roederer M. 2001. Spectral compensation for flow cytometry: Visualization artifacts, limitations, and caveats. Cytometry 45:194–205.

48. Shey MS, Hughes EJ, Kock M de, Barnard C, Stone L, Kollmann TR, Hanekom WA, Scriba TJ. 2012. Optimization of a whole blood intracellular cytokine assay for measuring innate cell responses to mycobacteria. J Immunol Methods 376:79–88.

49. Bosshart H, Heinzelmann M. 2011. Spontaneous decrease of CD14 cell surface expression in human peripheral blood monocytes ex vivo. J Immunol Methods 368:80–83.

50. Gorczyca W, Sun ZY, Cronin W, Li X, Mau S, Tugulea S. 2011. Immunophenotypic pattern of myeloid populations by flow cytometry. Methods Cell Biol 103:221-66.

51. Mcnab FW, Berry MPR, Graham CM, Bloch SAA, Oni T, Wilkinson KA, Wilkinson RJ, Kon OM, Banchereau J, Chaussabel D, O'Garra A. 2011. Programmed death ligand 1 is over-expressed by neutrophils in the blood of patients with active tuberculosis. Eur J Immunol 41:1941–1947.

52. Van Kooten C. 2000. Immune regulation by CD40-CD40-L interactions-2; Y2K update. Front Biosci 5:D880-693.

53. Alderson MR, Armitage RJ, Tough TW, Strockbine L, Fanslow WC, Spriggsr MK. 1993. CD40 expression by human monocytes: Regulation by cytokines and activation of monocytes by the ligand for CD40. J Ex Med 178(2):669–674.

54. Maecker HT, Frey T, Nomura LE, Trotter J. 2004. Selecting fluorochrome conjugates for maximum sensitivity. Cytometry part A 62:169–173.

55. Kleeman B, Olsson A, Newkold T, Kofron M, DeLay M, Hildeman D, Grimes HL. 2018. A guide to choosing fluorescent protein combinations for flow cytometric analysis based on spectral overlap Cytometry A 93(5):556-562.

56. Kagina BMN, Abel B, Scriba TJ, Hughes EJ, Keyser A, Soares A, Gamieldien H, Sidibana M, Hatherill M, Gelderbloem S, Mahomed H. Specific T cell frequency and cytokine expression profile do not correlate with protection against tuberculosis after bacillus Calmette-Guérin vaccination of newborns. Am J Respir Crit Care Med 182(8):1073-9.

57. Nylander S, Kalies I. 1999. Brefeldin A, but not monensin, completely blocks CD69 expression on mouse lymphocytes: Efficacy of inhibitors of protein secretion in protocols for intracellular cytokine staining by flow cytometry. J Immunol Methods 224:69–76.

58. Soares A, Govender L, Hughes J, Mavakla W, de Kock M, Barnard C, Pienaar B, Janse van Rensburg E, Jacobs G, Khomba G, Stone L, Abel B, Scriba TJ, Hanekom WA. 2010. Novel application of Ki67 to quantify antigen-specific in vitro lymphoproliferation. J Immunol Methods 362:43–50.

59. Kiritsy MC, Mccann K, Mott D, Holland SM, Behar SM, Sassetti CM, Olive AJ. Mitochondrial respiration contributes to the interferon gamma response in antigen-presenting cells. Elife 10:e65109.

60. Niedergang F, Hemar A, Hewitt CRA, Owen MJ, Dautry-Varsat A, Alcover A. 1995. The *Staphylococcus* aureus enterotoxin B superantigen induces specific T cell receptor down-regulation by increasing its internalization. J Biol Chem 270:12839–12845.

61. Shey MS, Randhawa AK, Bowmaker M, Smith E, Scriba TJ, de Kock M, Mahomed H, Hussey G, Hawn TR, Hanekom WA. 2010. Single nucleotide polymorphisms in toll-like receptor 6 are associated with altered lipopeptide and mycobacteria-induced interleukin-6 secretion. Genes Immun 11:561–572.

62. Shah JA, Musvosvi M, Shey M, Horne DJ, Wells RD, Peterson GJ, Cox JS, Daya M, Hoal EG, Lin L, Gottardo R, Hanekom WA, Scriba TJ, Hatherill M, Hawn TR. 2017. A functional toll-interacting protein variant is associated with Bacillus Calmette-Guerin-specific immune responses and tuberculosis. Am J Respir Crit Care Med 196:502–511.

63. Lippens C, Garnier L, Guyonvarc'h PM, Santiago-Raber ML, Hugues S. 2018. Extended freeze-dried BCG instructed pDCs induce suppressive Tregs and dampen EAE. Front Immunol 9:2777.

Appendix

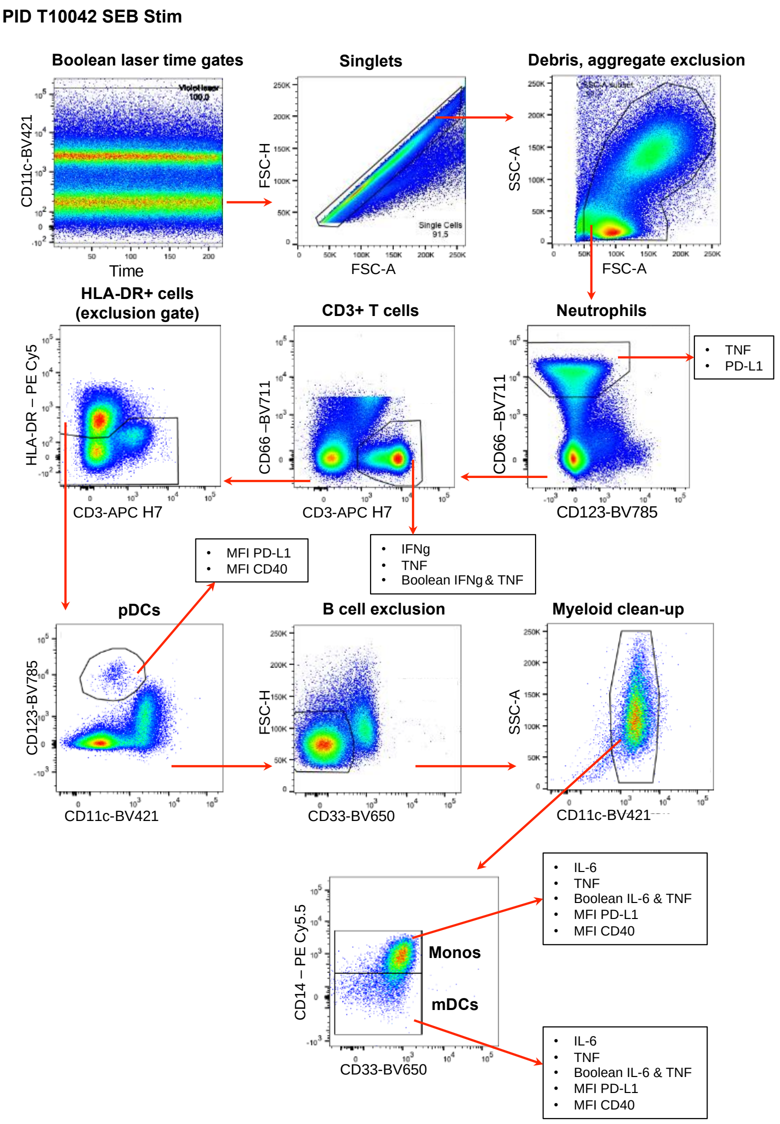

Figure A 1. ***Representative SEB stimulated sample gating strategy.*** The flow cytometric gating analysis deployed to elucidate consistent T cell, monocyte, myeloid and plasmacytoid dendritic cell and neutrophil populations across samples. This is a representative SEB stimulated sample from an infant (PID T10042). Time gates for each laser were set and Boolean gates used to ensure uniform fluorescence over time during acquisition. Doublets were excluded from the analysis by gating on FSC-height vs FSC-area. Total leucocytes were identified by the SSC-area vs FSC-area gate which excluded additional debris and/or large antibody aggregates. Neutrophils were identified as CD66a/c/e+ cells. The CD66a/c/e- population was used to identify CD3+ T cells. The resultant CD66-CD3- population was used to identify HLA-DR+ cells. pDCs were derived from this compartment and defined as HLA-DR+CD123+CD11c-. B cells were excluded by size and CD33 expression from the other myeloid cells of interest with a FSC-height vs CD33 gate. These myeloid cells were further cleaned up by using a SSC-area vs CD11c gate. Monocytes were separated from mDCs by the use of CD14. The relevant expression of intracellular cytokines and/or maturation markers was then determined on T cells, neutrophils, monocytes, pDCs and mDCs.

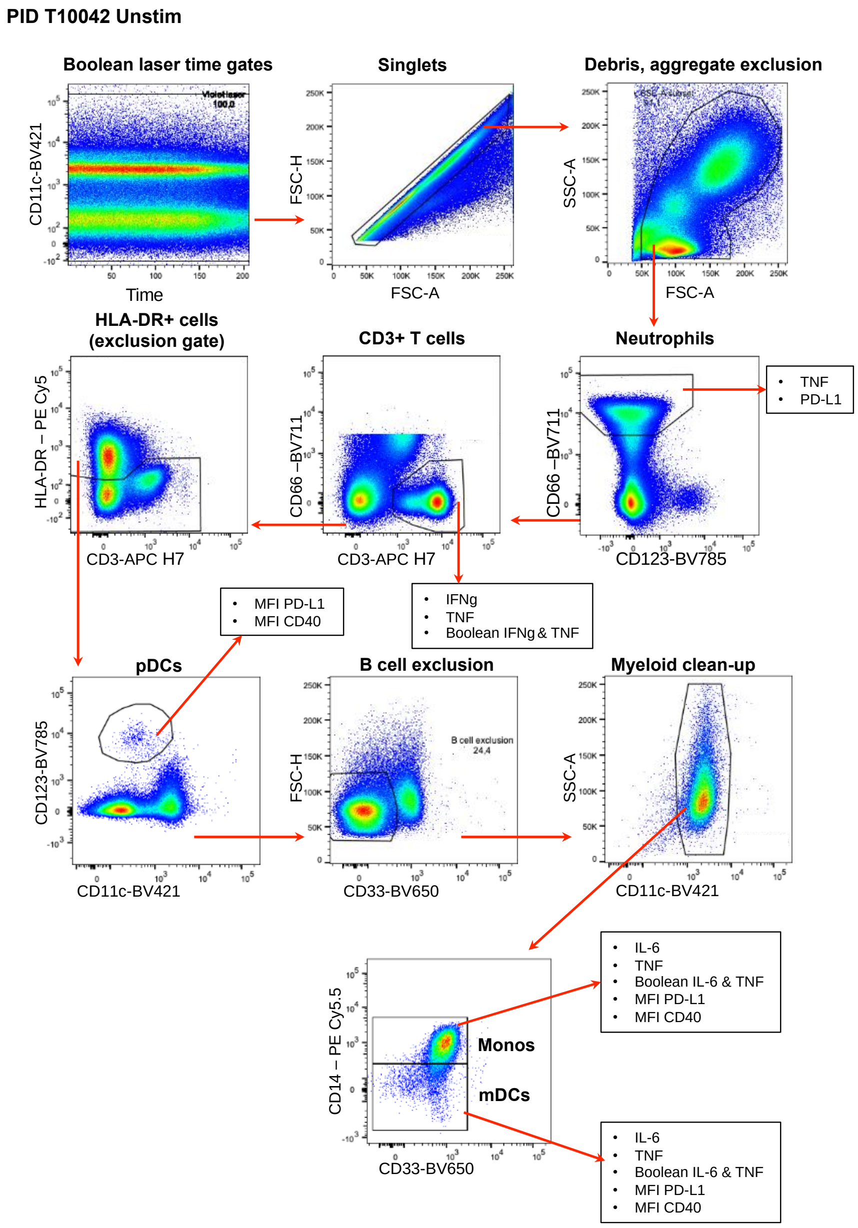

Figure A 2. ***Representative Unstimulated sample gating strategy.*** The flow cytometric gating analysis deployed to elucidate consistent T cell, monocyte, myeloid and plasmacytoid dendritic cell and neutrophil populations across samples. This is a representative unstimulated (unstim) sample from an infant (PID T10042). Time gates for each laser were set and Boolean gates used to ensure uniform fluorescence over time during acquisition. Doublets were excluded from the analysis by gating on FSC- height vs FSC-area. Total leucocytes were identified by the SSC-area vs FSC-area gate which excluded additional debris and/or large antibody aggregates. Neutrophils were identified as CD66a/c/e+ cells. The CD66a/c/e- population was used to identify CD3+ T cells. The resultant CD66-CD3- population was used to identify HLA-DR+ cells. pDCs were derived from this compartment and defined as HLA-DR+CD123+CD11c-. B cells were excluded by size and CD33 expression from the other myeloid cells of interest with a FSC-height vs CD33 gate. These myeloid cells were further cleaned up by using a SSC-area vs CD11c gate. Monocytes were separated from mDCs by the use of CD14. The relevant expression of intracellular cytokines and/or maturation markers was then determined on T cells, neutrophils, monocytes, pDCs and mDCs.

Table A 1. ***Participant characteristics.*** *Sex, race and birth weight (Kg) of the 25 10-week infant participants. All the infants received bacillus Calmette–Guérin (BCG) vaccination at birth. Highlighted infants were excluded from the analysis due to poor sample quality after an internal quality control process was applied.*

Participant	Sample ID	Sample collection date	Sex	Race	Birth Weight (Kg)
1	T10042	2001.10.17	M	unknown	2.691
2	T10245	2001.10.17	F	unknown	2.875
3	T11201	2001.12.05	F	coloured	2.337
4	T11679	2001.11.08	F	black	2.68
5	T12198	2002.01.15	F	coloured	3.62
6	T12324	2001.11.29	M	coloured	3.88
7	T12561	2002.01.07	F	coloured	3.02
8	T12869	2002.01.07	M	coloured	2.66
9	T12947	2002.01.30	M	coloured	2.379
10	T13043	2002.01.21	F	coloured	2.86
11	T14561	2003.09.10	F	unknown	4.258
12	T14937	2002.09.03	F	coloured	1.70
13	T14956	2002.09.25	F	coloured	3.56
14	T14970	2003.01.15	F	coloured	2.01
15	T15194	2003.03.26	F	coloured	2.515
16	T15249	2003.07.01	M	coloured	3.58
17	T15279	2003.01.16	F	coloured	3.25
18	T15647	2003.01.21	M	coloured	3.42
19	T15762	2002.09.09	M	black	3.80
20	T15929	2003.02.11	M	coloured	1.78
21	T15949	2003.03.25	F	coloured	3.58
22	T16259	2003.02.06	M	coloured	2.68
23	T16374	2003.01.21	M	coloured	3.22
24	T16379	2003.03.18	F	black	3.08
25	T16389	2003.06.10	M	coloured	2.38